PROCEEDINGS A

royalsocietypublishing.org/journal/rspa

Research

Cite this article: Dear AJ, Mahadevan L. 2025 Approximate Lie symmetries and singular perturbation theory. *Proc. R. Soc. A* **481**: 20240103.
https://doi.org/10.1098/rspa.2024.0103

Received: 7 February 2024
Accepted: 1 November 2024

Subject Category:
Mathematics

Subject Areas:
applied mathematics, differential equations, mathematical physics

Keywords:
singular perturbation theory, approximate Lie symmetry, renormalization group theory

Authors for correspondence:
Alexander J. Dear
e-mail: alexander.dear@bc.biol.ethz.ch
L. Mahadevan
e-mail: lmahadev@g.harvard.edu

Electronic supplementary material is available online at https://doi.org/10.6084/m9.figshare.c.7702285.

THE ROYAL SOCIETY PUBLISHING

Approximate Lie symmetries and singular perturbation theory

Alexander J. Dear[1,2] and L. Mahadevan[2]

[1]Department of Biology, Institute of Biochemistry, ETH Zurich, Otto Stern Weg 3, 8093 Zurich, Switzerland
[2]School of Engineering and Applied Sciences, Departments of Physics and of Organismic and Evolutionary Biology, Harvard University, Harvard, MA, USA

AJD, 0000-0003-3055-607X; LM, 0000-0002-5114-0519

Perturbation theory plays a central role in the approximate solution of nonlinear differential equations. However, its naïve application often yields divergent series solutions. While these can be made convergent using singular perturbation methods of various types, the procedures used can be subtle owing to the lack of globally applicable algorithms. Inspired by the fact that all exact solutions of differential equations are consequences of their (Lie) symmetries, we reformulate perturbation theory for differential equations as a series expansion of their solutions' symmetries. This is a change in perspective from the usual method of obtaining series expansions of the solutions themselves. We show that these approximate symmetries are straightforward to calculate and are never singular; their integration is therefore an easier way of constructing uniformly convergent solutions. This geometric viewpoint naturally subsumes the renormalization group-inspired approach of Chen, Goldenfeld and Oono, the method of multiple scales and the Poincare–Lindstedt method, by exploiting a fundamental class of symmetries that we term 'hidden scale symmetries'. It also clarifies when and why these singular perturbation methods succeed and just as importantly, when they fail. More broadly, direct, algorithmic identification and integration of these hidden scale symmetries permits solution of problems where other methods are impractical.

1. Introduction

How do we typically solve nonlinear differential equations (DEs) analytically? We guess a solution, or use various approximate methods that fall under the rubric of perturbation theory. The latter involve a whole range of methods but it is never clear which will work for which equation. Therefore, this would appear to be a laborious process, with uncertain chances of success. However, it is known that all exact solutions of arbitrary DEs, should they exist, can be approached via an algorithmic manner using the theory of continuous (Lie) symmetry groups [1]. (Indeed, even though today Lie theory finds application across diverse fields of the physical sciences, solving DEs was the original motivation for the development of the subject.) Lie theory reveals that in the cases where an exact solution to a DE can be found, the underlying property that is unconsciously or explicitly exploited is a Lie symmetry of the DE [2]. Furthermore the theory provides a single general integration procedure that can be applied to any arbitrary DE, in which Lie symmetries are first calculated algorithmically, and then leveraged to simplify or solve the DE using a small number of standard techniques.

Many DEs encountered in the physical sciences do not admit simple exact analytical solutions, regardless of the method used. Therefore, solving DEs approximately using perturbation theory is an important tool. This involves identifying a small parameter, ϵ, in the DEs such that they admit a simple analytical solution for $\epsilon = 0$. The dependent variable y is then solved for as a 'perturbation series' in ϵ, $y^{(0)} + \epsilon y^{(1)} + \cdots$ [3]. (ϵ can alternatively be an artificially introduced parameter that similarly reduces the DE to easily solvable form when set to zero, and that will later be set to 1 after the perturbation series has been obtained. In this guise, perturbation theory is sometimes also referred to as a 'homotopy method' or similar terminology [4]). A critical limitation of perturbation theory is that many problems are 'singular', defined as one whose perturbation series has a radius of convergence that vanishes somewhere within the region of phase space of interest [3]. To overcome this issue, there exist several 'singular perturbation methods' that convert divergent perturbation series into uniformly convergent approximate solutions [3,5,13]. Their implementation requires considerable intuition and it is challenging to determine *a priori* to which kinds of divergent series a given technique can be successfully applied.

This prompts us to ask the question: Just as (exact) Lie symmetries underpin most methods for the exact solution of DEs, could *approximate* Lie symmetries (appropriately defined) provide a rigorous and unified basis for the various singular perturbation methods used to approximately solve perturbed DEs? Equivalently, we ask if there is a natural approximate scheme inspired by the exact Lie-group inspired framework in quantum field theory [6] that led to modern renormalization group-based techniques (for a historical review, see [7]). From the perspective of this study that focuses on classical mechanics, the renormalization group-inspired method of Chen, Goldenfeld and Oono (CGO RG) [8,9] and its alternative formulation by Kunihiro (RG/E) [10,11] have been shown to equal or exceed in accuracy and generality earlier methods for regularizing singular perturbation series, being simpler than matched asymptotic expansions, and yielding an often faster route to finding the slow motion equations sought by multiple scales analysis and reductive perturbation techniques [12,13]. Discovering a Lie symmetry basis for these techniques would help rationalize their success, and could be used to understand more clearly under what circumstances they will be (in)applicable.

2. Structure of paper

For completeness, we provide in §3 a quick introduction to those aspects of the established Lie theory of differential equations that are needed in this article. In the electronic supplementary material, §S1, we also provide overviews of singular perturbation theory, the CGO RG method and its alternative RG/E formulation.

Our first result is the establishment of an algorithmic integration procedure for perturbed DEs based on approximate Lie symmetries, that yields convergent solutions (§4a). Next, in §4b, we

develop a simple and practical method for calculating approximate Lie symmetries of solutions to perturbed DEs, illustrating its application using the simple linear example of the overdamped linear oscillator. In §4c, we devise a transparent and general singular perturbation method based on exploiting a class of symmetries that we term 'hidden scale' symmetries. We showcase some of its advantages over other singular perturbation techniques in §4d by solving a fourth-order Turing-type pattern formation equation in a relatively straightforward manner.

In §4e, we next *derive* the CGO RG method, revealing it to simply be an indirect approach to identifying and exploiting hidden scale symmetries involving some trial-and-error. The celebrated solutions using CGO RG of the notorious 'switchback' problems, that would appear to contradict this Lie symmetry interpretation, are revisited in §4f and found to actually be *regular* perturbation series in a switching parameter entering the boundary conditions. The Oseen equations of fluid mechanics is found in §4f(ii) to be the regular first-order boundary condition perturbation of the steady incompressible Navier–Stokes equation, explaining its successful use to approximate the latter and allowing us to derive regular perturbative solutions for flow past a cylinder in the low-Reynolds limit.

We follow with a series of examples to which we apply the hidden scale symmetry method to further demonstrate its advantages and to reveal the basis in Lie symmetries of other popular techniques. First, we revisit the 'switchback' problems in §4g, this time to second order, to clarify using its Lie symmetry basis precisely why CGO RG sometimes finds exact solutions. Next, in §4h, we use the Mathieu equation as an example that is solved by the method of multiple scales (MMS). Solving directly by hidden scale symmetry reveals that MMS also seeks these hidden scale symmetries, but indirectly and often involving guesswork and/or additional effort. Following this, we explain in §4i the hidden scale symmetry basis of the Poincare–Lindstedt method (PLM). Consequently, we can determine guidelines around its applicability, which we illustrate with the Korteweg–de Vries (KdV) equation.

Finally, we use a modified Burgers equation to show in §4j that when these hidden scale symmetry-based methods fail, other classes of approximate symmetries can sometimes be similarly exploited to develop global solutions. We conclude in §5 with a discussion of several questions raised by the ideas introduced in this article.

3. Review of Lie point symmetries of differential equations

A point transformation is one that maps the independent and dependent variable values x and y of a mathematical object to new values $\tilde{x}$ and $\tilde{y}$. Point transformations that are indexed by at least one arbitrary parameter s may be written $\tilde{x} = \tilde{x}(x, y, s),\ \tilde{y} = \tilde{x}(x, y, s)$. When these are also invertible, contain the identity at $s = 0$ and obey $\tilde{x}(\tilde{x}(x, y, s), \tilde{y}(x, y, s), t) = \tilde{x}(x, y, s + t)$, they form a one-parameter (or multi-parameter) group of point transformations.

Such transformations have the useful property that they are continuous, and can best be visualized as motion along lines in phase space that are parameterized by s, which are known as the orbits of the group. Generalizing to multiple independent and dependent variables represented by $\boldsymbol{x} = (x_1, x_2, \dots)$ and $\boldsymbol{y} = (y_1, y_2, \dots)$, we can obtain the infinitesimal transformations for the group by expanding around $s = 0$:

$$\tilde{x}_i(\boldsymbol{x}, \boldsymbol{y}, s) = x_i + s\,\xi_i(\boldsymbol{x}, \boldsymbol{y}) + O(s^2), \quad \tilde{y}_j(\boldsymbol{x}, \boldsymbol{y}, s) = y_j + s\,\eta_j(\boldsymbol{x}, \boldsymbol{y}) + O(s^2) \tag{3.1a}$$

$$\xi_i(\boldsymbol{x}, \boldsymbol{y}) = \left.\frac{\partial \tilde{x}_i}{\partial s}\right|_{s=0}, \quad \eta_j(\boldsymbol{x}, \boldsymbol{y}) = \left.\frac{\partial \tilde{y}_j}{\partial s}\right|_{s=0}. \tag{3.1b}$$

$(\xi_1, \dots, \xi_n, \eta_1, \dots, \eta_m)$ forms the tangent vector to these orbits at $(\boldsymbol{x}, \boldsymbol{y})$. We can rewrite the

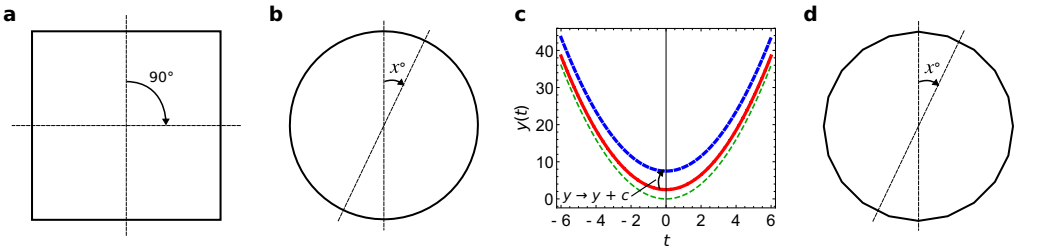

Figure 1. An overview of Lie symmetries. (a) Squares have discrete rotational symmetries. These cannot be reduced to infinitesimal form; therefore, they are not Lie symmetries. (b) Circles can be rotated by any amount; rotation is thus a Lie symmetry of the circle. (c) In general, symmetries of DEs map solutions to other solutions with different boundary conditions. An arbitrary translation on the y axis is a Lie symmetry of the DE $\dot{y} = 2t$, because this is solved by $y = t^2 + c$, and the translation just changes the value of c, giving the solution to the DE for new boundary conditions. (d) Dodecagons are only approximately invariant under infinitesimal rotational transformations (to $O(\varepsilon)$, where $\varepsilon \sim z \cos\theta$, with θ the external angle and z the side length), which are therefore an approximate Lie symmetry.

transformation as:

$$\tilde{x}_i(\boldsymbol{x}, \boldsymbol{y}, s) = x_i + s\,\boldsymbol{X}x_i + O(s^2), \quad \tilde{y}_j(\boldsymbol{x}, \boldsymbol{y}, s) = y_j + s\,\boldsymbol{X}y_j + O(s^2), \tag{3.2a}$$

$$\boldsymbol{X} = \sum_i \xi_i(\boldsymbol{x}, \boldsymbol{y}) \frac{\partial}{\partial x_i} + \sum_j \eta_j(\boldsymbol{x}, \boldsymbol{y}) \frac{\partial}{\partial y_j}. \tag{3.2b}$$

The operator $\boldsymbol{X}$ is the infinitesimal generator of the point transformation and completely characterizes it. Integrating the tangent vector over s will yield a finite transformation, i.e. a non-infinitesimal motion along an orbit. Now we can define a Lie point symmetry of an object as a continuous point transformation that leaves the object invariant (figure 1*a*,*b*). Other kinds of Lie symmetry exist, involving different kinds of continuous transformations, but we need not consider them here.

Any Lie symmetries of the arbitrary differential equation $F(\boldsymbol{x}, \boldsymbol{y}, \nabla \boldsymbol{y}, \nabla\nabla \boldsymbol{y}, \dots) = 0$ must thus satisfy

$$\boldsymbol{X}F = 0, \quad \text{wherever } F = 0. \tag{3.3}$$

(This can also be written in shorthand as $\boldsymbol{X}F|_{F=0} = 0$.) All symmetries can be fully specified by solving equations (3.2*b*)–(3.3) for $\xi_i(\boldsymbol{x}, \boldsymbol{y})$ and $\eta_j(\boldsymbol{x}, \boldsymbol{y})$ and subsequently constructing $\boldsymbol{X}$ from them. Although this is an essentially algorithmic procedure it is often extremely laborious, because applying $\boldsymbol{X}$ to the derivatives within F is highly complicated. Fortunately, we can omit the technical details of transforming derivatives here, because directly solving equation (3.3) is unnecessary in the present work. In §3, we instead develop vastly simpler alternative approaches for computing the symmetries we need. In any case, nowadays solving equation (3.3) is usually automated using packages available for computer algebra systems (CAS) such as Mathematica, although such automation can fail when F contains more than three variables.

There exist several established methods for integrating or simplifying DEs using their symmetries; however, only one is relevant enough to this article to merit a description here. Lie symmetries of differential equations transform solutions to other solutions (figure 1*c*). Thus, if a special solution for a differential equation is known, families of group-invariant solutions may be found by identifying the Lie symmetries of the parent DE and applying the corresponding finite transformations to this special solution. As a very brief illustration of this, it may be easily found by CAS that the heat equation $u_t - u_{xx} = 0$ admits several point symmetries, one of which is

$$\boldsymbol{X} = xt\frac{\partial}{\partial x} + t^2\frac{\partial}{\partial t} - \left(\frac{x^2}{4} + \frac{t}{2}\right)u\frac{\partial}{\partial u}. \tag{3.4}$$

Integrating an infinitesimal symmetry generator over a finite distance in parameter space leads to finite symmetry transformations, i.e. parameterizations of the symmetry's orbits, motions along which leave the DE invariant. They can be computed by solving $\boldsymbol{X}J = 0$ for general J using the method of characteristics. For this particular symmetry, J is constant along characteristics defined by

$$\frac{d\tilde{x}}{ds} = \tilde{x}\tilde{t}, \quad \frac{d\tilde{t}}{ds} = \tilde{t}^2, \quad \frac{d\tilde{u}}{ds} = -\left(\frac{\tilde{x}^2}{4} + \frac{\tilde{t}}{2}\right)\tilde{u}, \tag{3.5}$$

(where s can be interpreted as the group parameter). Integrating from $(s, \tilde{t}, \tilde{x}, \tilde{u}) = (0, t, x, u)$ yields

$$\tilde{x} = x/(1 - st), \quad \tilde{t} = t/(1 - st), \quad \tilde{u} = u\sqrt{1 - st}e^{-sx^2/4(1-st)}. \tag{3.6}$$

The t- and x-transformations may be inverted to give

$$t = \tilde{t}/(1 + s\tilde{t}) \Rightarrow 1 - st = 1/(1 + s\tilde{t}) \tag{3.7}$$

$$x = \tilde{x}(1 - st) = \tilde{x}/(1 + s\tilde{t}). \tag{3.8}$$

They may then be combined with the forward u-transformation to give

$$\tilde{u} = \frac{u}{\sqrt{1 + s\tilde{t}}}e^{-s\tilde{x}^2/4(1+s\tilde{t})}. \tag{3.9}$$

Applying this to the special solution of the heat equation $u = A$, where A is an arbitrary constant, yields the group-invariant solution (dropping the tildes):

$$u = \frac{A}{\sqrt{1 + st}}e^{-sx^2/4(1+st)}, \tag{3.10}$$

and s is now another arbitrary constant. (Note, albeit not relevant to this study, probably the most common method for exploiting the Lie symmetries of DEs is instead the construction of similarity solutions for PDEs from the invariants of their symmetry transformations.)

Finally, most of the established literature deals with exact symmetries of DEs, whose transformations leave them entirely unchanged. A more recent insight [14] is that the symmetry generator $\boldsymbol{X}$ of a perturbed DE $F = F_0 + \epsilon F_1 = 0$ can be expanded in powers of ϵ. Truncating this series $\boldsymbol{X} = \boldsymbol{X}^{(0)} + \epsilon\boldsymbol{X}^{(1)} + \ldots$ yields 'approximate symmetries', that leaves the DE invariant up to a given order in ϵ (figure 1*d*). They can be identified by solving

$$(\boldsymbol{X}^{(0)} + \epsilon\boldsymbol{X}^{(1)} + \ldots)(F_0 + \epsilon F_1)|_{F_0+\epsilon F_1=0} = 0, \tag{3.11a}$$

$$\Rightarrow O(\epsilon^0): \quad \boldsymbol{X}^{(0)}F_0|_{F_0=0} = 0, \tag{3.11b}$$

$$O(\epsilon^1): \quad \boldsymbol{X}^{(0)}F_1|_{F_0=0} + \boldsymbol{X}^{(1)}F_0|_{F_0=0} + \epsilon^{-1}\boldsymbol{X}^{(0)}F_0|_{F_0+\epsilon F_1=0} = 0, \ \cdots \tag{3.11c}$$

order-by-order in ϵ [15]. Systems that do not admit exact solutions may admit such approximate symmetries, which can then be used to integrate approximately the DEs to yield approximate solutions.[1] However, they are more technically challenging to calculate than exact symmetries, and few or no CAS packages can fully automate this procedure.

4. Results

(a) Approximate Lie symmetry is a natural language for perturbation theory

In geometric terms, the fundamental aim of singular perturbation theory is to construct a manifold that approximates everywhere within the phase space of interest to $O(\epsilon^k)$ the manifold spanned

[1]Note alternative approaches for their computation have been proposed [16,17] and there is some debate as to which is superior [17,18].

by the exact solution to a perturbed DE with perturbation parameter ϵ (figure 2*a*). Perturbation theory in the traditional sense (expanding the dependent variable as a power series in ϵ) only finds such approximate manifolds if this series happens to be regular. Otherwise, it finds a manifold that coincides only locally with an approximate manifold (figure 2*b*). By contrast, $O(\epsilon^k)$ expansions of the *Lie symmetries* of the solution to a perturbed DE (approximate Lie symmetries [14,15]) must encode transformations that map both exact and approximate manifolds to themselves to $O(\epsilon^k)$ *globally*. A specific $O(\epsilon^k)$ approximate manifold is moreover left exactly invariant by a given $O(\epsilon^k)$ approximate symmetry.

This gives us the idea of constructing globally valid approximate solutions to a perturbed DE by explicitly identifying and exploiting an approximate solution symmetry. The orbits of such symmetries describe pathways running along the associated approximate manifold, obtained by repeated transformation of a given starting point on the manifold. Therefore, transforming with this symmetry a special solution valid at one value of this coordinate should yield a global approximate solution. The power of this approach can be greatly increased by treating nominally constant parameters in the problem as independent variables, and looking for approximate solution symmetries that act on them. Not only does this increase the likelihood of a suitable symmetry existing (that we term approximate '*extended* symmetries'), but it also makes easier the identification of a suitable special solution to transform, which can now be e.g. a solution valid when one of the constant parameters is set to zero.

(b) Approximate solution symmetries can be calculated directly from the perturbation series

The solutions to a DE admit symmetries that the DE itself does not and vice versa. The computation of solution symmetries, exact or approximate, has hitherto been done by applying standard techniques of Lie analysis to the DEs themselves, either with auxiliary 'differential constraints' [19], or with a subsequent 'restriction' step to eliminate unwanted degrees of freedom associated with non-fixed initial or boundary conditions [20]. Unfortunately, both approaches can be extremely computationally challenging, even with the aid of CAS, particularly for approximate extended symmetries; moreover, neither approach can reliably find all solution symmetries.

Fortunately, if a perturbation series solution with arbitrary integration constants is available (a 'bare' perturbation series), it proves possible to compute *approximate* solution symmetries in a much more direct manner, with minimal calculations required. The manifold of a singular perturbation series calculated to $O(\epsilon^k)$ locally approximates the exact solution manifold to $O(\epsilon^k)$ near where the boundary or initial conditions are imposed, so the series must still locally be left invariant by the $O(\epsilon^k)$ approximate solution symmetries of the perturbed DE. But, if the integration constants, which we write as $\boldsymbol{A} = (A_1, A_2, \dots)$, are arbitrary then these conditions can be imposed anywhere. Therefore, by changing the values of these constants appropriately, the perturbation series can be made to act like a probe, locally satisfying the approximate solution symmetries at any desired region of the manifold (analogously to how microscopy works; figure 2*c*,*d*).

Therefore, instead of employing all the complicated mathematical machinery necessary to calculate the approximate symmetries of the parent differential equation (equation (3.11)), we can merely calculate the symmetries of the perturbation series, which must also be approximate symmetries of the exact solution. This is achieved by solving order-by-order the equation:

$$(\boldsymbol{X}^{(0)} + \epsilon \boldsymbol{X}^{(1)} + \cdots)(y - y^{(0)} - \epsilon y^{(1)} - \cdots)|_{y=y^{(0)}+\epsilon y^{(1)}+\dots} = 0, \tag{4.1a}$$

$$\Rightarrow O(\epsilon^0): \quad \boldsymbol{X}^{(0)}(y - y^{(0)})|_{y=y^{(0)}} = 0, \tag{4.1b}$$

$$O(\epsilon^1): \ \boldsymbol{X}^{(0)} y^{(1)}|_{y=y^{(0)}} - \boldsymbol{X}^{(1)}(y - y^{(0)})|_{y=y^{(0)}} - \frac{1}{\epsilon}\boldsymbol{X}^{(0)}(y - y^{(0)})|_{y=y^{(0)}+\epsilon y^{(1)}} = 0, \ \dots \tag{4.1c}$$

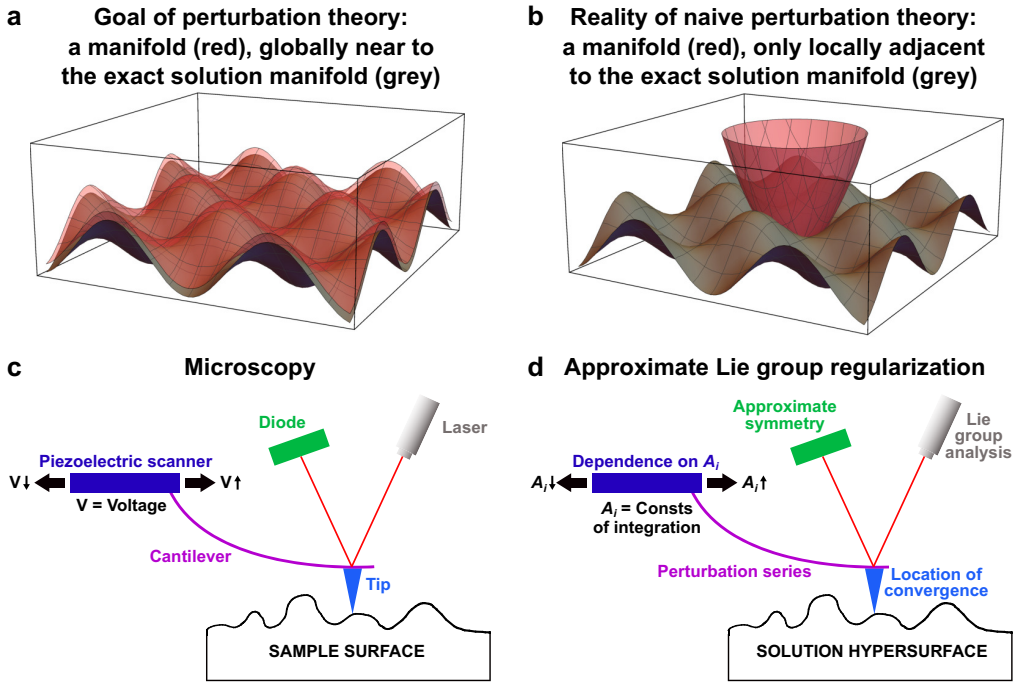

Figure 2. (a,b) Singular perturbation theory can be thought of in geometric terms, as an attempt to approximate the exact solution manifold (grey). (a) The goal is to construct a simple analytical solution whose manifold (red) is everywhere within ϵ of the exact manifold. (b) For singularly perturbed problems, a naive application of perturbation theory generates a manifold that coincides only locally with the exact manifold. (c,d) Analogy between our approximate Lie group regularization approach and microscopy. (Although we illustrate the analogy using atomic force microscopy (AFM), it also works for other kinds of microscopy such as optical microscopy.) (c) In AFM, the sample surface is scanned by the tip of a probe by changing the voltage of a piezoelectric scanner connected to the probe. The tip displacement is determined by detecting the deflection of a laser beam by the cantilever using a diode. A model of the surface can thus be built, whose resolution is given by the radius of the probe tip. (d) In our approximate Lie group approach, the solution hypersurface is scanned by the convergent region of a singular perturbation series in ε by changing the values of the constants of integration $\boldsymbol{A}$. The position in phase space of the point of convergence can be monitored during this process by approximate Lie group analysis and recorded in an approximate symmetry. An approximate solution can then be built from this symmetry, whose accuracy is given by the magnitude of ε.

where $y^{(i)}$ is the ith term in the naive perturbation series solution (for arbitrary initial or boundary conditions) to the differential equation $F(y, \boldsymbol{x}, \nabla y, ...) = 0$ (for dependent and independent variables y and $\boldsymbol{x}$).

The simplicity of this approach opens up new possibilities for Lie symmetry analysis. A key possibility is that this method can identify extended symmetries that act not just on the parameters entering the DEs, but also on parameters such as the integration constants $\boldsymbol{A}$ that enter solely the solutions. There is no way to do this by the traditional approach of identifying the symmetries of the parent differential equation. In particular, an approximate symmetry describing how the integration constants $\boldsymbol{A}$ change with x should in principle provide a global approximation of the exact solution anywhere on the manifold. To explore this hypothesis, and to demonstrate how equation (4.1) is solved in practice, we consider the overdamped harmonic oscillator for $t \geq 0$ and undefined initial conditions:

$$\epsilon \frac{d^2y}{dt^2} + \frac{dy}{dt} + y = 0, \quad \epsilon \ll 1. \tag{4.2}$$

Transforming into the inner region (i.e. boundary layer) by writing $\tau = \epsilon t$, this becomes

$$\frac{d^2y}{d\tau^2} + \frac{dy}{d\tau} + \epsilon y = 0. \tag{4.3}$$

Although it may be solved exactly, it is also a singular perturbation problem (figure 4*a*). Expanding y in ϵ as $y(\tau, \epsilon) = y^{(0)}(\tau) + \epsilon y^{(1)}(\tau) + O(\epsilon^2)$ yields the following perturbation equations to first order:

$$\frac{d^2y^{(0)}}{d\tau^2} + \frac{dy^{(0)}}{d\tau} = 0, \quad \frac{d^2y^{(1)}}{d\tau^2} + \frac{dy^{(1)}}{d\tau} + y^{(0)} = 0. \tag{4.4}$$

Solving without initial conditions yields the 'bare' perturbation series:

$$y_1(\tau) = A + Be^{-\tau} + \epsilon\left[-A\tau + B\tau e^{-\tau}\right], \tag{4.5}$$

where the subscript indicates a finite perturbation series $y_k = \sum_{i=0}^{k} \epsilon^i y^{(i)}$. The generator to first order in ϵ for a symmetry connecting A, B and τ has the form

$$\boldsymbol{X}_1 = \sum_{i=0}^{1} \epsilon^i \boldsymbol{X}^{(i)} = \sum_{i=0}^{1} \epsilon^i \left(\xi_A^{(i)} \frac{\partial}{\partial A} + \xi_B^{(i)} \frac{\partial}{\partial B} + \xi_\tau^{(i)} \frac{\partial}{\partial \tau}\right). \tag{4.6}$$

Since the magnitude of the tangent vector carries no information about the symmetry or its orbits, we can without loss of generality set its element in the τ-direction equal to 1, i.e. $\xi_\tau^{(i)} = \delta_{i,0}$. It should now be clear that solving equation (4.1) alone using equation (4.6) will *not* give a single symmetry that tells us how to update both A and B in response to an arbitrary change in τ. This is because only one degree of freedom is eliminated at each order, leaving either $\xi_A^{(i)}$ or $\xi_B^{(i)}$ also arbitrary. This issue is resolved by noting that a globally valid approximate symmetry should also leave the derivatives of the solution approximately invariant. Therefore, alongside equation (4.1), we also require

$$\boldsymbol{X}_1 \left(\dot{y} - \dot{y}_1\right)\big|_{\dot{y}=\dot{y}_1} = 0. \tag{4.7}$$

Solving equations (4.1) and (4.7) order-by-order in ϵ, we find at zeroth-order,

$$\boldsymbol{X}^{(0)} y^{(0)} = \xi_A^{(0)} + \xi_B^{(0)} e^{-\tau} - Be^{-\tau} = 0 \tag{4.8a}$$

$$\boldsymbol{X}^{(0)} \dot{y}^{(0)} = -\xi_B^{(0)} e^{-\tau} + Be^{-\tau} = 0 \tag{4.8b}$$

$$\therefore \xi_A^{(0)} = 0, \quad \xi_B^{(0)} = B. \tag{4.8c}$$

Then, at first order,

$$\boldsymbol{X}^{(0)} \dot{y}^{(1)} + \boldsymbol{X}^{(1)} \dot{y}^{(0)} = e^{-\tau}\left(-\xi_B^{(1)} - B\right) \tag{4.9a}$$

$$\boldsymbol{X}^{(0)} y^{(1)} + \boldsymbol{X}^{(1)} y^{(0)} = -A + Be^{-\tau} + \xi_A^{(1)} + \xi_B^{(1)} e^{-\tau} \tag{4.9b}$$

$$\therefore \xi_B^{(1)} = -B, \quad \xi_A^{(1)} = A. \tag{4.9c}$$

Pulling this together yields the generator of the anticipated $\boldsymbol{A}$–x symmetry:

$$\boldsymbol{X}_1 = \frac{\partial}{\partial \tau} + \epsilon A \frac{\partial}{\partial A} + B(1-\epsilon)\frac{\partial}{\partial B}. \tag{4.10}$$

Symmetries connecting integration constants and independent variables may seem unusual, but in fact, arbitrary transformations of the integration constants are clearly always symmetries of DEs. In this context, they are known as 'generalized symmetries' [1] or 'dynamical symmetries' [2], and are closely studied because they underpin Noether's theorem [1]. For symmetries instead of the solutions to DEs, the permissible transformations of the $\boldsymbol{A}$ are no longer arbitrary and we need new terminology. Since, as will become clear later, these symmetries find hidden scales, we refer to them hereafter as 'hidden scale symmetries'.

(c) General formulation of the 'hidden scale' symmetry method

As $\tau \to 0$, the divergent terms of the perturbation series equation (4.5) vanish, yielding a non-divergent special solution $y = A + B$. Because the generator equation (4.10) is valid globally to $O(\epsilon)$, so must be its orbits, given by

$$\frac{dA}{d\tau} = \epsilon A, \quad \frac{dB}{d\tau} = B(1-\epsilon). \tag{4.11}$$

These orbits can therefore be used to transform the non-divergent $\tau = 0$ solution into a global approximate solution. Therefore, integrating backwards from $\tau = \tau$ to $\tau = 0$ gives the finite transformation connecting $(A,\ B)$ at $\tau = 0$ with their values $(\tilde{A},\ \tilde{B})$ at $\tau = \tau$:

$$A = \tilde{A}e^{-\epsilon\tau}, \quad B = \tilde{B}e^{-(1-\epsilon)\tau}. \tag{4.12}$$

These orbits must be true to $O(\epsilon)$ for any τ; substituting into the non-divergent $\tau = 0$ solution $y = A + B$ thus provides a genuine global $O(\epsilon)$ perturbative solution to equation (4.3):

$$y(\tau) = \tilde{A}e^{-\epsilon\tau} + \tilde{B}e^{-(1-\epsilon)\tau} + O(\epsilon^2). \tag{4.13}$$

We will now derive a simplified but general formulation for this approach. In so doing, we will show that identifying and solving the finite transformation (FT) equations for hidden scale symmetries like this can be performed directly, with no need to explicitly calculate the symmetries themselves. Consider an arbitrary ODE with dependent and independent variables y and x. The element of the tangent vector of the kth-order hidden scale symmetry in the x direction may be chosen without loss of generality to equal 1. Its generator $\boldsymbol{X}_k(x, \boldsymbol{A})$ may thus be written

$$\boldsymbol{X}_k(x, \boldsymbol{A}) = \frac{\partial}{\partial x} + \sum_{i=1}^{n}\sum_{j=0}^{k} \epsilon^j \xi_{A_i}^{(j)} \frac{\partial}{\partial A_i}. \tag{4.14}$$

An invariant $J_k(x, \boldsymbol{A})$ of this approximate symmetry satisfies $\boldsymbol{X}_k(x, \boldsymbol{A})J_k(x, \boldsymbol{A}) = 0$. They are excellent approximate solutions because $J_k(x, \boldsymbol{A}) = y(x, \boldsymbol{A}) + O(\epsilon^{k+1})$ globally. The equation that gives this invariant $J_k(x, \boldsymbol{A})$ is

$$0 = \boldsymbol{X}_k(x, \boldsymbol{A})J_k = \frac{\partial J_k}{\partial x} + \sum_{i=1}^{n}\sum_{j=0}^{k} \epsilon^j \xi_{A_i}^{(j)} \frac{\partial J_k}{\partial A_i}. \tag{4.15}$$

From the method of characteristics this partial differential equation is reduced to $dJ_k/dx = 0$, i.e. $J_k =$ constant, along characteristics defined by

$$\sum_{j=0}^{k} \epsilon^j \xi_{A_i}^{(j)} = \frac{dA_i}{dx}. \tag{4.16}$$

Now, using this result in equation (4.14) yields

$$\boldsymbol{X}_k(x, \boldsymbol{A}) = \frac{\partial}{\partial x} + \sum_i \frac{dA_i}{dx} \frac{\partial}{\partial A_i}, \tag{4.17}$$

where the A_i are now functions of x that span the $J_k(x, \boldsymbol{A})$ invariant (the orbits of the symmetry). If we have not already computed the hidden scale symmetry then $\xi_{A_i}^{(j)}$ and thus dA_i/dx are not known. They may, however, be in principle calculated by observing that the perturbation series to order k, y_k, is left invariant by the hidden scale symmetry only in the limit $\epsilon \to 0$, i.e. $\boldsymbol{X}_k(x, \boldsymbol{A})y_k|_{\epsilon\to 0} = 0$. Thus the FT equation can be rewritten as

$$\left.\frac{\partial y_k}{\partial x}\right|_{\epsilon\to 0} + \sum_i \left.\frac{dA_i}{dx}\frac{\partial y_k}{\partial A_i}\right|_{\epsilon\to 0} = 0. \tag{4.18}$$

Equation (4.18) is underdetermined when there is more than one orbit to determine, i.e. more than one integration constant. This is resolved by requiring both the solution manifold and its

first $n-1$ derivatives to be left approximately invariant. Since these can be approximated at any location by the equivalent derivative of the perturbation series in the limit $\epsilon \to 0$, we solve the following equations for $j = [0, \dots, n-1]$:

$$\left.\frac{\partial^j y_k}{\partial x^j}\right|_{\epsilon\to 0} + \sum_{i=1}^{n} \frac{dA_i}{dx}\frac{\partial}{\partial A_i}\left.\frac{\partial^j y_k}{\partial x^j}\right|_{\epsilon\to 0} = 0. \tag{4.19}$$

This provides n equations for n unknowns, fully determining the system. To develop a uniformly convergent solution, a special value $x = x_0$ is first identified for which the divergences in the perturbative expansion vanish. Next, equations (4.18)–(4.19) are backward-integrated from arbitrary x to this value, i.e. integrated from $(x, \tilde{\boldsymbol{A}})$ to $(x_0, \boldsymbol{A}(x))$, where $\tilde{\boldsymbol{A}}$ are the integration constants associated with the FT equations. This procedure gives how $\boldsymbol{A}$ in the (convergent) perturbative expansion at $x = x_0$ must change with x to ensure this solution remains valid, and will be illustrated in subsequent examples. Following these prescriptions, equation (4.19) directly finds the simplest possible kth-order perturbative approximation to the solution manifold; that is, the invariant of the $O(\epsilon^k)$ hidden scale symmetry, which constitutes a globally valid $O(\epsilon^k)$ approximate solution.

To see how this is done in practice, consider the first-order perturbation series, equation (4.5) of the overdamped harmonic oscillator and its derivative:

$$y_1(\tau) = A + Be^{-\tau} + \epsilon\left[-A\tau + B\tau e^{-\tau}\right] \tag{4.20a}$$

$$\dot{y}_1(\tau) = -Be^{-\tau} + \epsilon\left[-A + B(1-\tau)e^{-\tau}\right]. \tag{4.20b}$$

Applying equation (4.19) results in the following equations for A and B to $O(\epsilon^2)$ (where we have used suffixes to indicate derivatives):

$$0 = A_\tau + (B_\tau - B)e^{-\tau} + \epsilon\left[-A_\tau\tau - A + B_\tau\tau e^{-\tau} + B(1-\tau)e^{-\tau}\right] \tag{4.21a}$$

$$0 = -(B_\tau - B)e^{-\tau} + \epsilon\left[-A_\tau + (B_\tau - B)(1-\tau)e^{-\tau} - Be^{-\tau}\right]. \tag{4.21b}$$

Adding these reveals that both $A_\tau = O(\epsilon)$ and $B_\tau - B = O(\epsilon)$, allowing the simplification:

$$0 = A_\tau + (B_\tau - B)e^{-\tau} + \epsilon\left[-A + Be^{-\tau}\right] \tag{4.22a}$$

$$0 = -(B_\tau - B)e^{-\tau} + \epsilon\left[-Be^{-\tau}\right]. \tag{4.22b}$$

These are none other than the FT equation (4.11) of the directly calculated $\boldsymbol{A} - x$ symmetry, as expected. As shown above, it can be applied to transform the convergent $\tau = 0$ special solution $A + B$ into a global solution.

The FT equations for the full $\boldsymbol{A} - x$ symmetry can sometimes be too complicated to solve analytically. This can sometimes be resolved by seeking instead the slow scale(s) symmetry only, which amounts to removing only the divergent terms from the perturbation series by symmetry transformation. This is done by relabelling only the divergent instances of x at first order and above as new variable μ, a process we refer to as 'painting'. Next, the FT equations (4.18)–(4.19) are still applied, but for dependent variable μ rather than x. Their solution is generally much easier, for two reasons. First, they no longer depend on the fast scale as well as the slow scale(s), so have a simpler form. Second, they are solved with the additional condition that $\boldsymbol{A}$ be independent of x. This reduces the number of derivatives of the perturbation series required to fully specify the symmetry, often to none. In the final step, the reverse substitution $\mu \to x$ is made, yielding the global approximate solution.

A key requirement for painting to be mathematically valid is that the painted series with arbitrary constants of integration remain a valid perturbation series for any value of μ. Otherwise, a symmetry calculated from the series will not be a globally valid approximate symmetry of the exact solution manifold. This necessitates that all painted divergent terms can be written $g(\mu)h(x)$, where h is one of the (convergent) fundamental solutions of the reference system. (For instance, in the example just considered, these are 1 and $e^{-\tau}$.) Then any change in μ can be compensated

for by a change in $\boldsymbol{A}$. We give more detailed methodological guidelines for painting, alongside their mathematical justification, in the electronic supplementary material, §S2. Finally, one can often simplify further the calculations by deleting all but the most divergent terms at each order prior to solving the FT equations, at the price of the resulting symmetry retaining full validity only asymptotically (also discussed later).

We illustrate how painting works in practice using again the perturbation series equation (4.5) of the overdamped harmonic oscillator, which becomes

$$y_1(\tau,\mu) = A + Be^{-\tau} + \epsilon\left[-A\mu + B\mu e^{-\tau}\right]. \tag{4.23}$$

Applying equation (4.19) yields

$$0 = A_\mu + B_\mu e^{-\tau} + \epsilon\left[-A_\mu\mu - A + (B_\mu\mu + B)e^{-\tau}\right]. \tag{4.24}$$

Requiring independence of $A(\mu)$ and $B(\mu)$ from τ, and noting that this implies $A_\mu,\ B_\mu = O(\epsilon)$, gives different FT equations:

$$\frac{dA}{d\mu} = \epsilon A, \qquad \frac{dB}{d\mu} = -\epsilon B. \tag{4.25}$$

However, the $\mu = 0$ convergent special solution $y = A + Be^{-\tau}$ is also different; transforming it by equation (4.25) results in the same global solution as before.

(d) Hidden scale symmetry method is especially well-suited for solving high-order ODEs

Higher-order ODEs give rise to multiple constants of integration, higher-order divergent terms in the perturbation series, and frequently unusual scales. This makes most other singular perturbation methods painstaking to implement, including CGO RG and MMS. Such problems are thus ideal for demonstrating the power and simplicity of the hidden scale symmetry method.

We consider the formation of localized deformations in a flexible filament that can swell or grow in length, but that is embedded in an elastic substrate, studied in [21]. These are described by sinusoidal displacements $\bar{W}$ perpendicular to the original alignment of the filament, modulated by a non-trivial envelope. Let the filament ends be anchored at $\bar{x} = \pm\bar{L}/2$, where $\bar{x}$ is the non-dimensional horizontal co-ordinate (and $\bar{L}$ the original filament length). Providing all other boundary conditions are chosen symmetrically around $\bar{x} = 0$, the system has a mirror symmetry. Then, starting from eqn (3.2) from [21] and restoring a term that was dropped for simplicity (see eqn [S53] from [21]), $\bar{W}$ is described for $0 \le \bar{x} \le \bar{L}/2$ by the following fourth-order DE:

$$(1 + \partial_{\bar{x}\bar{x}})^2\bar{W} - \delta\,\partial_{\bar{x}}\left(\frac{(\bar{x} - \bar{L}/2)^2}{2}\bar{W}_{\bar{x}}\right) = 0, \tag{4.26}$$

where $\delta \ll 1$ is the non-dimensional strain, and the solution for $-\bar{L}/2 \le \bar{x} \le 0$ can be constructed using the mirror symmetry around $\bar{x} = 0$. This is a Turing–Swift–Hohenberg-type equation, with the leftmost operator featuring frequently in equations describing pattern formation. (We use notation $\partial_{\bar{x}}\bar{W} = \partial\bar{W}/\partial\bar{x} = \bar{W}_{\bar{x}}$.)

Since CGO RG was not practical (see below), equation (4.26) was solved in [21] using MMS, requiring the extremely difficult guess of the existence of a hidden $\delta^{1/4}$(!) scale. However, it can be solved much more straightforwardly using hidden scale symmetry, as follows. Expanding $\bar{W}$ in δ as $\bar{W} = \bar{W}^{(0)} + \delta\bar{W}^{(1)} + O(\delta^2)$ yields perturbation equations:

$$(1 + \partial_{\bar{x}\bar{x}})^2\bar{W}^{(0)} = 0, \qquad (1 + \partial_{\bar{x}\bar{x}})^2\bar{W}^{(1)} = \partial_{\bar{x}}\left(\frac{(\bar{x} - \bar{L}/2)^2}{2}\bar{W}^{(0)}_{\bar{x}}\right). \tag{4.27}$$

The general solution with undetermined constants of integration for the zeroth-order term is

$$\bar{W}^{(0)}(\bar{x}) = A_1\cos\bar{x} + A_2\sin\bar{x} + \alpha_1\bar{x}\cos\bar{x} + \alpha_2\bar{x}\sin\bar{x}. \tag{4.28}$$

Although we could perform 'full' hidden scale analysis on $\bar{W}^{(0)} + \delta\bar{W}^{(1)}$, it proves much simpler to employ painting, i.e. replace divergent instances of x in $\bar{W}^{(1)}$ with μ and perform hidden scale

analysis on μ. Whatever higher order terms are painted, no convergent special solution is available for any value of μ unless $\alpha_1 = \alpha_2 = 0$. This allows solving equation (4.27) for $\bar{W}^{(1)}$ using only the terms $A_1 \cos\bar{x} + A_2 \sin\bar{x}$ for $\bar{W}^{(0)}$, greatly simplifying its form

$$\bar{W}^{(1)} = C(\bar{x})\cos\bar{x} + S(\bar{x})\sin\bar{x} \tag{4.29a}$$

$$C(\bar{x}, \boldsymbol{A}) = \frac{1}{192}\left[192(c_1 + \bar{x}c_2) + 12A_2(\bar{x}(\bar{L}^2/2 + 1) - \bar{L}/2)\right.$$
$$\left. + A_1(-9 + 6\bar{x}^2 + 2\bar{x}^4 + 6(\bar{L}/2)^2(2\bar{x}^2 - 3) - 2\bar{L}\bar{x}(2\bar{x}^2 + 3))\right] \tag{4.29b}$$

$$S(\bar{x}, \boldsymbol{A}) = \frac{1}{192}\left[192(c_3 + \bar{x}c_4) - 12A_1(\bar{x}(\bar{L}^2/2 + 1) - \bar{L}/2)\right.$$
$$\left. + A_2(-9 + 6\bar{x}^2 + 2\bar{x}^4 + 6(\bar{L}/2)^2(2\bar{x}^2 - 3) - 2\bar{L}\bar{x}(2\bar{x}^2 + 3))\right]. \tag{4.29c}$$

There are any number of ways the first-order integration constants c_i can be chosen to eliminate divergences at $O(\delta)$ arising from $\bar{x}$, rendering CGO RG impractical. Instead, we paint all divergent terms:

$$\bar{W}^{(0)} + \delta\bar{W}^{(1)} = (A_1 + \delta C(\mu, \boldsymbol{A}))\cos\bar{x} + (A_2 + \delta S(\mu, \boldsymbol{A}))\sin\bar{x}. \tag{4.30}$$

Applying equation (4.18) to $\bar{W}^{(0)} + \delta\bar{W}^{(1)}$, noting that $dS/d\mu = S_\mu + \sum_i S_{A_i} dA_i/d\mu = S_\mu + O(\delta)$ (and similarly for C) and insisting on independence from $\bar{x}$, leads to the following FT equations to $O(\delta)$:

$$0 = \partial_\mu A_1 + \delta C_\mu(\mu, \boldsymbol{A}), \qquad 0 = \partial_\mu A_2 + \delta S_\mu(\mu, \boldsymbol{A}) \tag{4.31a}$$

$$C_\mu(\mu, \boldsymbol{A}) = c_2 + \frac{A_2}{16}(\bar{L}^2/2 + 1) + \frac{A_1}{192}\left[12\mu + 8\mu^3 + 6\bar{L}^2\mu - 2\bar{L}(6\mu^2 + 3)\right] \tag{4.31b}$$

$$S_\mu(\mu, \boldsymbol{A}) = c_4 - \frac{A_1}{16}(\bar{L}^2/2 + 1) + \frac{A_2}{192}\left[12\mu + 8\mu^3 + 6\bar{L}^2\mu - 2\bar{L}(6\mu^2 + 3)\right]. \tag{4.31c}$$

These FT equations must now be backward-integrated, as explained above. However, we will want to solve them using a standard integral identity, which obviously requires forward integration. To reverse the direction of integration we must change the signs of all derivatives $\boldsymbol{A}_\mu$ in the FT equations, effectively reversing the direction of the orbit. In the present case, this means transforming equation (4.31) to

$$\partial_\mu A_1 = \delta C_\mu(\mu, \boldsymbol{A}), \qquad \partial_\mu A_2 = \delta S_\mu(\mu, \boldsymbol{A}). \tag{4.32}$$

Since $\boldsymbol{A}_\mu = O(\delta)$, differentiating equation (4.32) decouples them and gives the amplitude equations to $O(\delta)$:

$$\partial_{\mu\mu}\boldsymbol{A} = \delta\frac{\boldsymbol{A}}{16}\left[1 + 2(\mu - \bar{L}/2)^2\right]. \tag{4.33}$$

These equations are almost the same as the MMS equations [21] (and are identical if we consider only the most μ-divergent terms). They are solved by

$$\boldsymbol{A} = \tilde{\boldsymbol{A}} D\left[-\frac{1}{2} - \frac{2^{1/2}}{16}\delta^{1/2}, \frac{\delta^{1/4}}{2^{1/4}}(\bar{x} - \bar{L}/2)\right] + \tilde{\boldsymbol{B}}\, D\left[-\frac{1}{2} + \frac{2^{1/2}}{16}\delta^{1/2}, \mathrm{i}\cdot\frac{\delta^{1/4}}{2^{1/4}}(\bar{x} - \bar{L}/2)\right], \tag{4.34}$$

where $D[v, z]$ is the parabolic cylinder function and $\tilde{\boldsymbol{A}} = (\tilde{A}_1, \tilde{A}_2)$, $\tilde{\boldsymbol{B}} = (\tilde{B}_1, \tilde{B}_2)$ are the integration constants for equation (4.33). The symmetry of the system around $\bar{x} = 0$ provides the boundary conditions $\bar{W}'(\bar{x} = 0) = \bar{W}'''(\bar{x} = 0) = 0$; this requires that $\bar{W}$ have no dependence on $\sin\bar{x}$, i.e. $\tilde{A}_2 = \tilde{B}_2 = 0$. Requiring the solution to be real and to shrink as $\bar{x} \to \bar{L}/2$ further requires that $\tilde{B}_1 = 0$. We can therefore finally write $\bar{W}$ as

$$\bar{W}(\bar{x}) = \tilde{A}_1\, D\left[-\frac{1}{2} - \frac{2^{1/2}}{16}\delta^{1/2}, \frac{\delta^{1/4}}{2^{1/4}}(\bar{x} - \bar{L}/2)\right]\cos(\bar{x}). \tag{4.35}$$

We plot equation (4.35) in figure 3; it describes the slow amplitude modulation of sinusoidal buckling in the elastic filament. As strain increases the amplitude modulation becomes steeper and the buckling becomes more localized towards the centre of the filament.

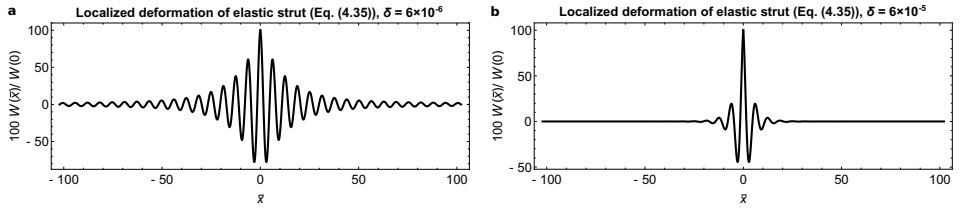

Figure 3. Plots of the growth-induced vertical buckling of an originally horizontal filament supported at each end and anchored in an elastic medium, for two different values of strain. Plots are constructed using equation (4.35) with $\bar{L} = 200$ for $\bar{X} \geq 0$ and its mirror image for $\bar{X} \leq 0$. (a) At small values of excess strain, the filament buckles into an approximately sinusoidal shape, with only a modest amplitude modulation. (b) Larger values of excess strain are accommodated by much stronger amplitude modulation, resulting in strongly localized buckling around the centre of the filament.

Since the approximate Lie symmetry used to generate this solution is $O(\delta)$, equation (4.35) is accurate to $O(\delta)$. It is almost identical to eqn (3.5) of [21] but with a correction $\propto \delta^{1/2}$ to the first argument of $D[v, z]$. This discrepancy arises because the term proportional to $\bar{x} - \bar{L}/2$ in the original DE (equation (4.26)) was dropped in [21] to simplify the MMS calculations. It was established that this term would contribute to the weakly nonlinear analysis to $O(\delta^{3/4})$, whereas all other terms contributed at $O(\delta^{1/2})$ or lower. Thus, although permissible to omit it, doing so restricted the accuracy of the resultant solution to $O(\delta^{1/2})$. By contrast, omitting this term would not meaningfully simplify the already fairly straightforward hidden scale calculations.

(e) CGO RG and RG/E are indirect methods for exploiting hidden scale symmetry

Equation (4.18) resembles the CGO RG equation (equation S1; see the electronic supplementary material, §S1B, for an introduction to CGO RG). It differs only in that the differentiation is with respect to x rather than x_0 or μ, and in that the limit $x \to x_0$ has been replaced by the limit $\epsilon \to 0$. This suggests that CGO RG may have a basis in approximate solution symmetries connecting the redundant parameter x_0 and $\boldsymbol{A}$. This can be true only if x_0 is introduced in a manner such that the divergent series remains a valid perturbative expansion with arbitrary integration constants and yields an exact, non-divergent special solution when $x \to x_0$. Otherwise, its approximate symmetries are not symmetries of the exact solution, and *cannot* give rise to a globally valid approximate solution. Since under these circumstances, CGO RG has been shown to find the envelope of the family of perturbation series with different x_0 [10], we call these 'envelope symmetries'.

To prove that this is indeed the case, we now derive the CGO RG equation from the finite transformation equations for envelope symmetries. The generator $\boldsymbol{X}_k(x_0, \boldsymbol{A})$ of the kth-order envelope symmetry may be written

$$\boldsymbol{X}_k(x_0, \boldsymbol{A}) = \frac{\partial}{\partial x_0} + \sum_{i=1}^{n} \sum_{j=0}^{k} \epsilon^j \xi_{A_i}^{(j)} \frac{\partial}{\partial A_i}, \tag{4.36}$$

where WLOG the element of the tangent vector in the direction of x_0 has been set to 1. An invariant $J_k(x, x_0, \boldsymbol{A})$ of this approximate symmetry satisfies $\boldsymbol{X}_k(x_0, \boldsymbol{A}) J_k(x, x_0, \boldsymbol{A}) = 0$:

$$0 = \boldsymbol{X}_k(x_0, A) J_k = \frac{\partial J_k}{\partial x_0} + \sum_{i=1}^{n} \sum_{j=0}^{k} \epsilon^j \xi_{A_i}^{(j)} \frac{\partial J_k}{\partial A_i}. \tag{4.37}$$

From the method of characteristics, this partial differential equation is reduced to $dJ_k/dx_0 = 0$, i.e. $J_k =$ constant, along characteristics defined by

$$\sum_{j=0}^{k} \epsilon^j \xi_{A_i}^{(j)} = \frac{dA_i}{dx_0}. \tag{4.38}$$

Now, using this result in equation (4.36) yields

$$\boldsymbol{X}_k(x_0, \boldsymbol{A}) = \frac{\partial}{\partial x_0} + \sum_i \frac{dA_i}{dx_0}\frac{\partial}{\partial A_i}. \tag{4.39}$$

If we have not already computed the envelope symmetry then $\xi^{(j)}_{A_i}$ and thus dA_i/dx_0 are not known. They may, however, be in principle calculated by observing that the perturbation series to order k, y_k, is left invariant by the envelope symmetry only in the limit $x \to x_0$, i.e. $\boldsymbol{X}_k(x_0, \boldsymbol{A})y_k|_{t\to t_0} = 0$. Thus

$$\left.\frac{\partial y_k}{\partial x_0}\right|_{x\to x_0} + \sum_i \frac{dA_i}{dx_0}\left.\frac{\partial y_k}{\partial A_i}\right|_{x\to x_0} = 0, \tag{4.40}$$

which is none other than the CGO RG equation.

This provides a highly intuitive explanation for *why* the seemingly trivial CGO RG equation should give globally valid approximate solutions: it is equivalent to the FT equations, valid globally, for the approximate symmetry connecting integration constants $\boldsymbol{A}$ and initial value x_0. When integrated from a known point on the exact solution manifold, the resultant finite transformation or orbit of this symmetry is necessarily a global approximate solution manifold of the desired order in ϵ. This also implies that the 'envelopes' that form the mathematical heart of RG/E [10,11,22] are exactly equivalent to the orbits of these approximate symmetries. In support of this viewpoint, it has previously been observed (although not to our knowledge proved generally) that the CGO RG equation has the structure of an asymptotic expansion of a Lie group generator [23]. The meaning of this result in terms of approximate symmetry properties of the exact solution was not investigated at the time.

What is the precise relationship between hidden scale symmetries and the envelope symmetries that we have shown underlie CGO RG and its alternative formulation, RG/E? To answer this, we will use again the overdamped linear oscillator, transformed into the inner region (equation (4.3)):

$$\frac{d^2y}{d\tau^2} + \frac{dy}{d\tau} + \epsilon y = 0, \tag{4.41}$$

and its first-order perturbative solution equation (4.5):

$$y_1(\tau) = A + Be^{-\tau} + \epsilon\left[-A\tau + B\tau e^{-\tau}\right]. \tag{4.42}$$

Now, in the original CGO formulation, one is free to 'split' the divergent terms using τ_0 however one sees fit, and redefine A, B to absorb the resulting terms dependent on τ_0 only, to ensure the τ-dependent terms vanish at $\tau = \tau_0$. $A\tau$ can only become $\tau - \tau_0$. For $B\tau e^{-\tau}$, however, there are an infinite number of choices, and in its most general form the split perturbation series becomes

$$y_1(\tau, \tau_0) = A + Be^{-\tau} + \epsilon\left[-A(\tau - \tau_0) + B(\tau e^{-\tau} - s\tau_0 e^{-\tau_0} - (1-s)\tau_0 e^{-\tau})\right], \tag{4.43}$$

where s can take any value.

Applying the CGO RG equation (equation (4.40)), for arbitrary s, yields

$$\Big(A_{\tau_0} + B_{\tau_0}e^{-\tau} + \epsilon\Big[A - A_{\tau_0}(\tau - \tau_0) + B(-se^{-\tau_0} + s\tau_0 e^{-\tau_0} - (1-s)e^{-\tau}) + B_{\tau_0}(\tau e^{-\tau} - s\tau_0 e^{-\tau_0} - (1-s)\tau_0 e^{-\tau})\Big]\Big)\Big|_{\tau\to\tau_0} = 0. \tag{4.44}$$

Now the limit $\tau \to \tau_0$ is invariably used in the literature to remove divergent terms proportional to $\tau - \tau_0$. In CGO RG, to prevent underdetermination, independence of the integration constants from τ is also demanded. However, since the integration constants are assumed to have τ_0

dependence and since in this limit τ is no longer independent from τ_0, this is apparently inconsistent. Instead, we are left with the doubly underdetermined equation:

$$A_{\tau_0} + B_{\tau_0} e^{-\tau_0} + \epsilon \left[A + B(s\tau_0 e^{-\tau_0} - e^{-\tau_0})\right] = 0, \tag{4.45}$$

where $A(\tau_0), B(\tau_0)$ and s are unknown. The correct solution (equation (4.13); figure 4*a*) can be arrived at by setting $s = 0$ and then partitioning terms in A and terms in B into separate equations [9]. But, how can we justify these steps mathematically?

To make progress we first remark that equation (4.45) generates the orbits of not one but a family of envelope symmetries satisfied by the perturbation series, only one member of which can be a symmetry of the exact solution. Each splitting s can thus be interpreted as a different way to parameterize the perturbation series into a family of adjacent curves, each with its own infinite set of envelopes, only one of which provides a valid global solution. Since the final step is to replace τ_0 with τ, this must be the one corresponding to the hidden scale symmetry. As in the hidden scale method, to identify it we must consider also the derivative of the splitted perturbation series equation (4.43):

$$\frac{dy_1(\tau, \tau_0)}{d\tau} = -Be^{-\tau} + \epsilon \left[-A + B(e^{-\tau} - \tau e^{-\tau} + (1-s)\tau_0 e^{-\tau})\right]. \tag{4.46}$$

The reason that only $s = 0$ gives the correct splitting is now revealed to be that only when $s = 0$ does the divergence in both equations (4.43) and (4.46) vanish as $\tau \to \tau_0$. Setting $s = 0$ and applying the CGO RG equation (equation (4.40)) then yields $A_{\tau_0} = B_{\tau_0} = O(\epsilon)$ and thus, in combination with equation (4.45):

$$A_{\tau_0} + B_{\tau_0} e^{-\tau_0} + \epsilon \left[A - Be^{-\tau_0}\right] = 0, \qquad -B_{\tau_0} e^{-\tau_0} + \epsilon \left[Be^{-\tau_0}\right] = 0. \tag{4.47}$$

By eliminating underdetermination, this gives the desired separation of terms in A and B, recovering the equations [9].

Thus, CGO RG and RG/E are effectively indirect methods to identify and exploit hidden scale symmetries, requiring introduction of an arbitrary τ_0 or x_0. CGO RG yields the envelope symmetries of the perturbation series; the one that is an inverted hidden scale symmetry and therefore yields a correct solution must be identified by trial-and-error and by guesswork. By contrast, in RG/E one is meant to convert nth-order ODEs into n first-order ODEs prior to application of the RG equation. This prevents underdetermination analogously to imposing equation (4.19) and also avoids potential inconsistencies introduced by requiring independence from τ, leading to an inverted hidden scale symmetry without guesswork.

(f) Key 'singular' problems are actually regular boundary condition perturbations

An important apparent success of the CGO RG method is its generation of unprecedentedly accurate solutions to the challenging 'switchback' family of problems, with vastly less effort than was required using older approaches. However, the derivations of these solutions appear inconsistent with a Lie group origin for CGO RG, and incompatible with RG/E [10,11]. In this section, we pause our exploration of Lie group methods to resolve this apparent paradox by utilizing an unusual and interesting perturbative technique.

(i) The switchback problems and their first-order solutions

The method of matched asymptotic expansions, a widely used singular perturbation technique, was first given mathematical foundations in the 1950s by Kaplun and Lagerstrom [24], and further developed by them and others in the 1960s [12], with the help of a family of particularly challenging model problems, known as switchback problems, that are asymptotically similar to

low Reynolds number problems. A minimal model for them is given by [25]:

$$\frac{d^2u}{dx^2} + \frac{n-1}{x}\frac{du}{dx} + u\frac{du}{dx} + \delta\left(\frac{du}{dx}\right)^2 = 0, \tag{4.48a}$$

$$u(x=\epsilon) = 0, \qquad u(x=\infty) = 1. \tag{4.48b}$$

n is interpretable as the dimension of the space, ϵ the radius of the sphere or circle inserted at the origin and $u(x=\infty)=1$ the velocity of the undisturbed fluid flow. These problems with $n=2,3$ and $\delta=0,1$ were also employed in a pedagogical context as a 'worst-case scenario' for the difficulty of applying matched asymptotic expansions in Hinch's textbook [13]. Equation (4.48) is already expressed in terms of the 'inner variable' x associated with the boundary layer at infinity [3,25]. In [8], equation (4.48) with $n=3,\ \delta=0$ was solved using CGO RG, with the intent to demonstrate the advantages of CGO RG over matched asymptotics. In Ref. [9], the same was done for equation (4.48) with $n=2,\ \delta=0,1$; in [25] this calculation was revisited in more detail. Indeed, the solutions found were both more accurate than the matched asymptotic solution of Hinch [13], and calculated far more easily.

In all cases, the reference system could not be solved fully, since setting $\epsilon=0$ simplifies neither the DE nor the boundary conditions. (The sphere or circle does not actually vanish, as the $u=0$ boundary condition remains even in this limit; instead, it becomes a no-slip point disturbance.) Instead, the partial reference solution $u^{(0)}=A=$ const. was used as a starting point to construct a *partial* perturbation series in ϵ, by expanding $u(x,\epsilon)=A+\sum_{i=1}\epsilon^i u^{(i)}(x)$, yielding at first order $u(x)=u_1(x,\epsilon)+O(\epsilon^2)$, where:

$$u_1(x) = A + \epsilon B e_2(x) \qquad (n=3,\ \delta=0) \tag{4.49a}$$

$$u_1(x) = A + \epsilon B e_1(x) \qquad (n=2,\ \delta=0,1), \tag{4.49b}$$

where $e_n(t)=\int_t^\infty d\rho\rho^{-n}e^{-\rho}$. These are not perturbation series in ϵ as they cannot satisfy the boundary conditions at each order in ϵ. Nonetheless, CGO RG was successfully applied, yielding

$$u(x) = 1 - \frac{e_2(x)}{e_2(\epsilon)} + O(\epsilon^2) \qquad (n=3,\ \delta=0) \tag{4.50a}$$

$$u(x) = 1 - \frac{e_1(x)}{e_1(\epsilon)} + O(\epsilon^2) \qquad (n=2,\ \delta=0,1). \tag{4.50b}$$

Note these are the same as the original perturbation series with constants A, B chosen to match the boundary conditions. These successes would thus appear to violate our Lie theoretic principle that CGO RG can only be applied to valid perturbation series solutions.

Trusting in our Lie theoretic interpretation of CGO RG implies that these partial series must still be valid perturbation series solutions despite appearances. This can only be true if the solutions were actually expanded in an artificial perturbation parameter a, which has subsequently been set to 1. (Note not all researchers classify series solutions in such artificial parameters as perturbative expansions; however, we will do so.) For this to succeed, $u_0=A=$ constant must be capable of satisfying the boundary conditions at zeroth-order. This in turn requires that the perturbation parameter a enters the boundary conditions rather than the DEs, in a way that $a=0$ reduces both boundary conditions to $u=1$. Therefore, the switchback problem can be formulated as a 'boundary condition perturbation':

$$\frac{d^2u}{dx^2} + \frac{n-1}{x}\frac{du}{dx} + u\frac{du}{dx} + \delta\left(\frac{du}{dx}\right)^2 = 0, \tag{4.51a}$$

$$u(x=\epsilon) = 1-a, \qquad u(x=\infty) = 1. \tag{4.51b}$$

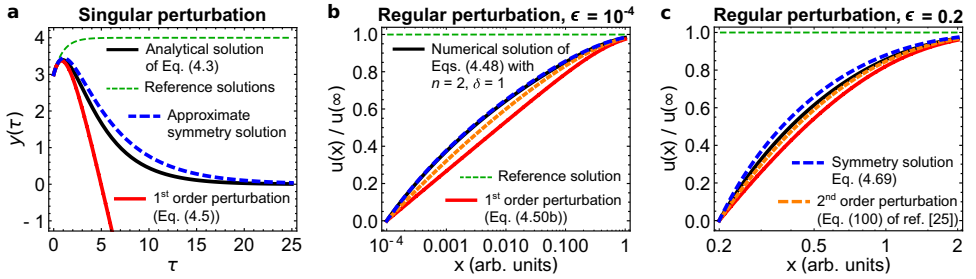

Figure 4. Regular versus singular perturbation problems. (a) The overdamped harmonic oscillator yields a singular perturbation series (equation (4.5)). This diverges for values of τ sufficiently far from where initial conditions were imposed. It is easier to regularize this using the hidden scale FT equation equation (4.18) than the CGO RG equation. Shown: $\epsilon = 0.2$, $y(0) = 3$, $y'(0) = 1$. (b,c) By contrast, the 'switchback' equations, equation (4.48), yield regular perturbation series in a switching parameter a for the small-x boundary condition (equations (4.51)–(4.54)). These series converge globally on the exact solution as higher-order terms are added, even when $a = 1$. Shown: $n = 2$, $\delta = 1$, $a = 1$. (b) The hidden scale FT equation yields the exact $x \to 0$ asymptotic solution equation (4.69) (shown: $\epsilon = 10^{-4}$). At very small ϵ, this is the most accurate approximation of equations (4.59). (c) At larger but still small ϵ, the second-order perturbative solution is instead the more accurate.

Expanding $u = u^{(0)} + au^{(1)} + O(a^2)$ then yields the zeroth-order perturbation equation:

$$\frac{d^2u^{(0)}}{dx^2} + \frac{n-1}{x}\frac{du^{(0)}}{dx} + u^{(0)}\frac{du^{(0)}}{dx} + \delta\left(\frac{du^{(0)}}{dx}\right)^2 = 0, \tag{4.52a}$$

$$u^{(0)}(x=\epsilon) = 1, \qquad u^{(0)}(x=\infty) = 1, \tag{4.52b}$$

which is solved by $u^{(0)} = 1$. The first-order equation is then

$$\frac{d^2u^{(1)}}{dx^2} + \frac{n-1}{x}\frac{du^{(1)}}{dx} + u^{(0)}\frac{du^{(1)}}{dx} = 0, \tag{4.53a}$$

$$u^{(1)}(x=\epsilon) = -1, \qquad u^{(1)}(x=\infty) = 0, \tag{4.53b}$$

which is solved by

$$u^{(1)}(x) = -\frac{e_2(x)}{e_2(\epsilon)} \qquad (n=3,\ \delta=0) \tag{4.54a}$$

$$u^{(1)}(x) = -\frac{e_1(x)}{e_1(\epsilon)} \qquad (n=2,\ \delta=0,1). \tag{4.54b}$$

The solutions equation (4.50) are then revealed as the first order perturbation series in a, $u^{(0)} + au^{(1)}$, with $a = 1$ to recover the desired boundary condition. Furthermore, plotting the numerical solution to the 'terrible' problem (equation (4.48) with $n = 2$, $\delta = 1$) alongside its first- and second-order perturbative solutions in a (equations (4.50*b*) and (4.61)) with $a = 1$ unambiguously confirms the regular nature of this problem, and that the radius of convergence of the perturbation series is greater than 1 (figure 4*b*,*c*). That this is a *regular* perturbation in the boundary condition is also proved explicitly in the electronic supplementary material, §S3.

Since a is set to 1, it is not immediately clear how to evaluate the accuracy of the approximation. However, since $e_2(\epsilon)^{-1}$ and $e_1(\epsilon)^{-1}$ are $O(\epsilon)$ when ϵ is small, the first order term is actually $O(a\epsilon)$ (provided $x \nsim \epsilon$). Moreover, as shown in the electronic supplementary material, §S3, the kth-order term when $n = 2$, $\delta = 0, 1$ is $O(a^k e_1(\epsilon)^{-k})$, which becomes $O(\epsilon^k)$ after setting a to 1. Therefore, despite not being a perturbative series in ϵ, for all but the smallest values of x the error of the perturbative approximation to kth order is still $O(\epsilon^{k+1})$.

(ii) The Navier–Stokes equations and the Oseen equation

We suspect that the identification of *regular* perturbations (or homotopies) in the boundary conditions as singular perturbation problems may have occurred frequently in the past (e.g. the problem studied in [26]); their re-evaluation may resolve several apparent paradoxes in the literature. As above, such problems in fact need not be treated by singular perturbation techniques or Lie group analysis at all. An example of significance is the incompressible steady Navier–Stokes equation of fluid mechanics:

$$u \cdot \nabla u = \nu \nabla^2 u - \frac{1}{\rho} \nabla p. \tag{4.55}$$

u and p are the (incompressible) velocity and pressure fields, ρ the liquid density and $\nu \propto 1/R$ the kinematic viscosity, for Reynolds number R. The Oseen equation is a famous and highly successful low-Reynolds number approximation of this equation:

$$U \cdot \nabla u = \nu \nabla^2 u - \frac{1}{\rho} \nabla p, \tag{4.56}$$

with boundary conditions (U is the (constant) bulk fluid velocity):

$$u(r) = 0 \quad r \in \text{ surface of fixed body}, \quad \lim_{|r| \to \infty} u(r) = U, \quad \lim_{|r| \to \infty} p(r) = p_\infty. \tag{4.57}$$

The Oseen equation was originally obtained from equation (4.55) by replacing u with $U + u^{(1)}$, without, in our view, a clear view of a perturbation parameter. Our work in this section, however, implies that the correct perturbation parameter to use is a, where the first boundary condition has been modified to

$$u(r) = U(1 - a) \quad r \in \text{surface of fixed body}. \tag{4.58}$$

Now the Oseen equation is a true first-order perturbation equation, and the perturbation series can match the boundary conditions precisely at each order in a.

It has been observed [27] that only for $R <\sim 1$ is this approximation valid near the body surface. This is presumably because the radius of convergence of the resultant perturbation series is dependent on R (and likely also on the body geometry). Only for $R <\sim 1$ does the radius of convergence exceed 1, so that the imposition of the no-slip boundary condition $u = 0$ at the body surface qualifies as a regular perturbation (or homotopy). This would also explain why the Oseen equation is always a valid approximation far enough from the body. For any R there should exist a surface r^* in the flow sufficiently far from the body that the exact $u(r^*)$ can be formulated as a perturbed 'surface' boundary condition $u(r^*) = U(1 - a)$ where a is within the radius of convergence of the regular perturbation series for the particular choice of R.

To illustrate in more detail how the Oseen equation can give rise to regular perturbative solutions to the Navier–Stokes equations, we consider in the electronic supplementary material, §S4, the classic problem of flow past an infinite cylinder, with 'no-slip' boundary conditions at the cylinder surface (remarking that flow past a sphere can be treated in a similar fashion). Expanding its Navier–Stokes equation in boundary condition parameter a, the corresponding Oseen equation is then revealed to be the first-order perturbation equation when a is set to 1. We also show that a well-known solution via CGO RG to the Oseen equation for this problem [25] is none other than the *regular* first-order boundary condition perturbation series in a for the corresponding Navier–Stokes equation.

(g) Singular perturbation methods can find exact solutions if the underlying hidden scale symmetries are exact

In this section, we return to the hidden scale symmetry method and demonstrate that it can be productively applied even to regular perturbation series if the underlying symmetry is a finite

polynomial in the perturbation parameter. In such cases, the method can generate exact solutions from low-order perturbation series.

The 'terrible' problem (equation (4.51) with $n=2,\ \delta=1$) is:

$$\frac{d^2u}{dx^2}+\frac{1}{x}\frac{du}{dx}+u\frac{du}{dx}+\left(\frac{du}{dx}\right)^2=0, \tag{4.59a}$$

$$u(x=\epsilon)=1-a, \qquad u(x=\infty)=1. \tag{4.59b}$$

Expanding u in a as before, but adding a second-order term, i.e. $u=u^{(0)}+au^{(1)}+a^2u^{(2)}+O(a^3)$, the second order perturbation equation is:

$$\frac{d^2u^{(2)}}{dx^2}+\frac{1}{x}\frac{du^{(2)}}{dx}+u^{(0)}\frac{du^{(2)}}{dx}=-u^{(1)}\frac{du^{(1)}}{dx}-\left(\frac{du^{(1)}}{dx}\right)^2, \tag{4.60a}$$

$$u^{(2)}(x=\epsilon)=0, \qquad u^{(2)}(x=\infty)=0. \tag{4.60b}$$

Solving equation (4.52) for unspecified boundary conditions gives us $u^{(0)}=A$. Solving equation (4.53) then gives $u^{(1)}=c_1+Be_1(Ax)$. Using these to solve equation (4.60), and keeping only the most divergent terms at each order, finally gives the regular second-order perturbation series:

$$u=A+aBe_1(Ax)-\frac{a^2}{2}B^2e_1(Ax)^2+O(a^3). \tag{4.61}$$

Changing variables for simplicity to $\tau=e_1(Ax)$, the perturbation series and its derivative become

$$u(\tau)=A+aB\tau-\frac{a^2}{2}B^2\tau^2+O(a^3), \qquad u'(\tau)=aB-a^2B^2\tau+O(a^3). \tag{4.62}$$

Applying the hidden scale FT equation to these gives

$$0=A'+a(B'\tau+B)-a^2(BB'\tau^2+B^2\tau)+O(a^3), \tag{4.63a}$$

$$0=B'-aB^2-2aBB'\tau+O(a^2), \tag{4.63b}$$

where A, B now depend on τ. Since equation (4.63b) gives $B'=O(a)$, these yield the FT equations:

$$B'=aB^2+O(a^2), \qquad A'=-aB+O(a^2). \tag{4.64}$$

The convergent special solution is $u=A$ at $\tau=0$ (corresponding to $x=\infty$). Therefore, we backward integrate from $(\tau,A,B)=(\tau,\tilde{A},\tilde{B})$ to $(0,A(\tau),B(\tau))$, yielding

$$B(\tau)=\frac{\tilde{B}}{1+a\tilde{B}\tau}+O(a^2), \tag{4.65a}$$

$$A(\tau)-\tilde{A}=-a\int_\tau^0 B(\tau)d\tau=\ln\left[1+a\tilde{B}\tau\right]+O(a^3). \tag{4.65b}$$

Therefore, switching variables back from τ to x, the hidden scale general solution is

$$\begin{aligned} u(x)=A(x)&=\tilde{A}+\ln\left[1+a\tilde{B}e_1(A(x)x)\right]+O(a^2)\\ &=\tilde{A}+\ln\left[1+a\tilde{B}e_1(\tilde{A}x)\right]+O(a^2). \end{aligned} \tag{4.66}$$

The boundary condition $u(x=\infty)=1$ implies that $\tilde{A}=1$. $\tilde{B}$ is obtained by satisfying the boundary condition $u(x=\epsilon)=1-a$:

$$1-a=1+\ln\left[1+a\tilde{B}e_1(\epsilon)\right]\Rightarrow a\tilde{B}=\frac{e^{-a}-1}{e_1(\epsilon)}. \tag{4.67}$$

Substituting into equation (4.65*b*), we recover

$$u(x) = 1 + \ln\left[1 - (1 - e^{-a})\frac{e_1(x)}{e_1(\epsilon)}\right] + O(a^3). \tag{4.68}$$

Setting $a = 1$ finally gives our hidden scale solution (figure 4*b*,*c*):

$$u(x) = \ln\left(e + (1 - e)\frac{e_1(x)}{e_1(\epsilon)}\right). \tag{4.69}$$

In the electronic supplementary material, §S3, we show that equation (4.68) is the exact sum of the most divergent terms in the perturbation series, to infinite order. Therefore, the hidden scale symmetry method has not identified an approximate solution, but instead the asymptotic $\epsilon \to 0$ limit of the *exact* solution to the 'terrible' problem. Equation (4.69) is thus better than the full second order perturbation solution (eqn (100) from [25]), but only when ϵ is small enough to justify losing the least divergent terms as $x \to \epsilon$ at second order (figure 4*b*,*c*).

Hidden scale analysis and CGO RG can find exact solutions only if the underlying hidden scale symmetry is exact. To be identifiable order-by-order by CGO RG or our hidden scale method, this symmetry must also be a finite power series in the perturbation parameter. Indeed, CGO RG to first order solves the nonlinear problem of Carrier exactly [9] because the exact envelope symmetry is linear in ϵ. In the present case, CGO RG or hidden scale symmetry analysis finds the asymptotic behaviour of the exact solution because the hidden scale symmetry is *asymptotically* a first-order polynomial in a as $x \to 0$, that can be discovered by CGO RG from the second-order perturbation series alone.

Veysey *et al.* [25] also treated the second-order perturbation series using CGO RG, and found multiple possible ways to perform the splitting step. Each possibility had to be investigated in turn, and only one ultimately led to Equation (4.69), with some others giving insoluble RG equations, and yet others returning the original perturbation series unchanged. The hidden scale symmetry method fortunately avoids this trial-and-error. (Veysey *et al.* ultimately opted to use the unchanged perturbation series as the most accurate, although as explained above, this is only true for larger values of ϵ.)

(h) Hidden scale symmetry origin of the method of multiple scales

In the MMS, the dependent variable is assumed to depend on extra slow scales $\tau_i = \epsilon^i t$, where $i > 0$ are guessed, and τ_i are treated as independent variables. Because, at zeroth-order, the perturbation equation is unchanged by introducing these additional scales, its solution is identical to the naive reference solution but with integration constants replaced by functions of these additional scales. Their functional form is subsequently chosen to ensure the secular terms at higher order vanish [3,13].

To illustrate the relationship between hidden scale symmetries and the method of multiple scales, we consider the Mathieu equation (treated by MMS on p. 560 [3]):

$$\ddot{y} + (a + 2\epsilon\cos t)y = 0. \tag{4.70}$$

It can be shown that for $a \neq n^2/4$ $(n = 0, 1, 2, \ldots)$, $y(t) = 0$ is stable for sufficiently small ϵ [3]. Investigating the stability boundary of solutions in the (a, ϵ) plane around $a = 1/4$ may be done by expanding a as $a(\epsilon) = 1/4 + a_1\epsilon + a_2\epsilon^2 + \ldots$. Expanding y similarly as $y = y^{(0)} + \epsilon y^{(1)}$ yields the perturbation equations to first order:

$$\ddot{y}^{(0)} + \frac{1}{4}y^{(0)} = 0, \quad \ddot{y}^{(1)} + (a_1 + 2\cos t)y^{(1)} = 0. \tag{4.71}$$

Solving these yields the first-order perturbation series:

$$y_1(t) = R\cos(t/2+\theta) + \epsilon A\cos(t/2+\theta) + \epsilon B\sin(t/2+\theta) + \epsilon R\left[\frac{1}{2}\cos(3t/2+\theta) + \sin(2\theta)t\cos(t/2+\theta) - (\cos(2\theta)+a_1)t\sin(t/2+\theta)\right], \quad (4.72)$$

where A and B are integration constants.

In this example, painting is essential to obtain FT equations simple enough to solve. The $t=0$ solution is a function of $\cos\theta$ and $\sin\theta$, but the full solution contains non-divergent terms proportional to $\cos(t/2+\theta)$ and $\cos(3t/2+\theta)$. A $t-\theta$ approximate symmetry converting the former into the latter would be very complex and likely non-analytic. Indeed, explicit computation of such a symmetry proves not to be possible in this case.

Painting equation (4.72) by replacing only divergent instances of t with a new variable μ yields

$$y_1(t) = R\cos(t/2+\theta) + \epsilon A\cos(t/2+\theta) + \epsilon B\sin(t/2+\theta) + \epsilon R\left[\frac{1}{2}\cos(3t/2+\theta) + \sin(2\theta)\mu\cos(t/2+\theta) - (\cos(2\theta)+a_1)\mu\sin(t/2+\theta)\right]. \quad (4.73)$$

Now, the FT equation can be applied for independent variable μ instead of t. (See the electronic supplementary material, Appendix S2, for why painting additionally some but not all convergent terms would have been inconsistent.) This recovers the same equations as are obtained by CGO RG [9], but time-inverted as expected due to the different direction of integration:

$$O(\epsilon) = R_\mu\cos(t/2+\theta) - R\sin(t/2+\theta)\theta_\mu \quad (4.74a)$$

$$\therefore O(\epsilon^2) = R_\mu\cos(t/2+\theta) - R\sin(t/2+\theta)\theta_\mu + \epsilon R\left[\sin(2\theta)\cos(t/2+\theta) - (\cos(2\theta)+a_1)\sin(t/2+\theta)\right] \quad (4.74b)$$

$$= R_\mu + \epsilon R\sin(2\theta) \quad = \theta_\mu + \epsilon(\cos(2\theta)+a_1). \quad (4.74c)$$

The solutions to these FT equations (eqns (2.16)–(2.18) from [9]) are plotted alongside numerical solutions to equation (4.70) in the electronic supplementary material, figure S1.

That CGO RG finds the same scales as multiple-scale analysis was discussed in [8,9]. It should now be clear that the correspondence in outcomes between these two techniques follows, like their validity, from their mathematical underpinning in hidden scale symmetries. CGO RG, MMS and the hidden scale symmetry method all find a globally convergent solution in the form of the convergent terms of the perturbation series with the zeroth-order integration constants replaced by slowly varying functions of the independent variables. The hidden scale symmetry method ensures this convergence rigorously and algorithmically by determining these functions through a globally valid symmetry transformation. In MMS, by contrast, guesswork is needed to identify the slow scales upon which these functions depend.

(i) Lie symmetry interpretation of the Poincare–Lindstedt method

The method of strained coordinates, or PLM, replaces independent variable t with $Q(\epsilon)t$, where $Q = 1 + q_1\epsilon + q_2\epsilon^2 + \ldots$. Similarly to MMS, the q_i are then chosen so that secular terms in the perturbation series $y_k = \sum_{i=1}^{k}\epsilon^i y^{(i)}$ vanish. From the Lie symmetry viewpoint, this is equivalent to introducing a switching parameter μ in front of the divergent terms in the perturbation series, where μ can run from 0 to 1, alongside the introduction of Q as outlined above, seeking an approximate symmetry connecting Q and μ, and expanding the resultant finite transformation to finite order in ϵ.

This viewpoint allows us to understand when PLM will succeed. Clearly, the perturbation series with arbitrary Q must still be a valid perturbative solution, which (since integration constants $\boldsymbol{A}$ can be chosen arbitrarily) in turn requires $y_k(t,\boldsymbol{A}) = y_k(f(t,A_1),\{A_{i>1}\}) = y_k(f(Qt,\tilde{A}_1),$

$\{A_{i>1}\}) + O(\epsilon^{k+1})$. In this case, PLM just looks for the finite transformation of a hidden scale symmetry involving only A_1, and will succeed only when such a symmetry exists. A second condition for the applicability of PLM is thus that the FT equations are zero to the desired order for all $\{A_{i>1}\}$.

As an example, we look at the travelling wave solutions of the KdV equation investigated [5] by PLM. A version of the KdV equation is

$$u_t + u_x + \frac{\delta^2}{6}u_{xxx} + \varepsilon\frac{3}{2}uu_x = 0. \tag{4.75}$$

Looking for a travelling wave solution $u = W(\theta) \equiv W(kx - \omega t)$ reduces this to an ODE:

$$(k-\omega)W' + \frac{\delta^2 k^3}{6}W''' + \varepsilon k\frac{3}{2}WW' = 0, \tag{4.76}$$

where prime notation here refers to differentiation with respect to θ. Expanding $W = W^{(0)} + \epsilon W^{(1)} + \epsilon^2 W^{(2)} + O(\epsilon^3)$, the reference solution $W_0 = W^{(0)}$ is obtained by solving

$$(k-\omega)(W^{(0)})' + \frac{\delta^2 k^3}{6}(W^{(0)})''' = 0, \tag{4.77}$$

yielding:

$$W_0 = R\sin(\lambda\theta + \phi) + c_0, \quad \lambda^2 = \frac{6(k-\omega)}{\delta^2 k^3}. \tag{4.78}$$

To restrict our attention to zero-average solutions, we set $c_0 = 0$. Next, WLOG we can set $\lambda = 1$, as [5], since λ just multiplies the arbitrary ω and k in equation (4.78). In the electronic supplementary material, §S5A, we calculate the terms in the resultant perturbation series to second order as:

$$W_2 = R\sin(\theta+\phi) - \varepsilon\frac{6R^2\sin\left(\frac{\theta}{2}\right)^3\sin\left(\frac{\theta}{2}+2\phi\right)}{k^2\delta^2} - \varepsilon^2\frac{27R^3\theta(6\cos(2\phi)-1)\cos(\theta+\phi)}{16k^4\delta^4} + \varepsilon^2\mathcal{R}, \tag{4.79}$$

where $\mathcal{R}$ consists of all the non-divergent functions in the second-order term (and is given in the electronic supplementary material, equation S32).

We can now compute the $O(\epsilon^2)$ convergent approximate solution using hidden scale symmetries. Using initial conditions $W(0) = W''(0) = 0,\ W'(0) = A_1$ this yields (see the electronic supplementary material, §S5B):

$$W(\theta) = A_1\sin((1-q)\theta) + \frac{3\varepsilon A_1^2}{4k^2\delta^2}\left[4\cos((1-q)\theta) - \cos(2(1-q)\theta) - 3\right] \tag{4.80a}$$

$$q = \frac{135A_1^2\varepsilon^2}{16k^4\delta^4}. \tag{4.80b}$$

Since the hidden scale solution has the same form of the PLM ansatz, PLM is clearly also applicable here. In the textbook [5], PLM is implemented in a surprising way, in which only t is modified, not θ. This is mathematically equivalent thanks to the arbitrariness of ω, and may be re-expressed as a modification for θ by calculating how it modifies λ from 1 (see the electronic supplementary material, §S5C). Adapting for the initial conditions $W(0) = W''(0) = 0,\ W'(0) = A_1$ yields the same expression for W, but with q replaced by

$$q_{\text{text}} = \frac{27A_1^2\varepsilon^2}{16k^5\delta^4}, \tag{4.81}$$

i.e. differing to our solution by a factor of $1/(5k)$ in q. Plotting against the numerical solution confirms the solution in the textbook is incorrect whereas our solution is correct (figure 5).

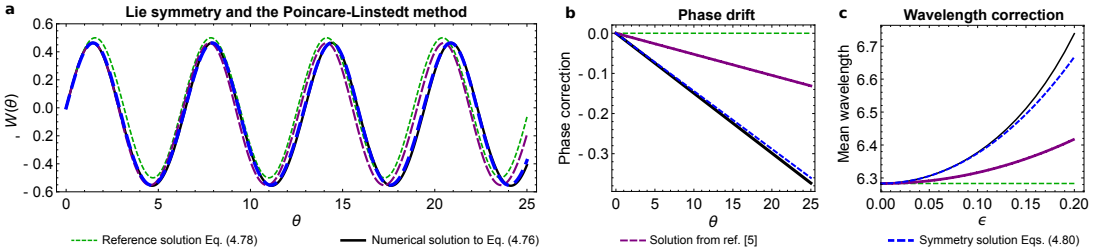

Figure 5. The method of strained coordinates is not always applicable. (a) Travelling wave solutions of the Korteweg–de Vries equation satisfy equation (4.76), which admits a singular perturbation series. This was solved incorrectly by the Poincare–Lindstedt method [5]; here, it is easily solved correctly by the hidden scale symmetry method ($\epsilon = 0.14,\ W(0) = W''(0) = 0,\ W'(0) = 0.5$). (b) The error in the solution from ref. [5] becomes more apparent at larger θ, because (c) the source of the error is an incorrect modification to the wavelength. The second-order hidden scale symmetry solution holds the correct wavelength up until $\epsilon \simeq 0.15$.

(j) Other symmetries can sometimes be exploited when hidden scale symmetries are intractable

Sometimes these methods yield an insoluble RG or FT equation. An example of where this occurs is the modified inviscid Burgers equation as an initial-value problem:

$$u_t + \epsilon u u_x^2 = 0, \quad u(t_0, x) = U(t_0, x), \tag{4.82}$$

where $U(t_0, x)$ is an arbitrary initial value. (We can later impose a known initial value at $t_0 = 0$.) Expanding u in ϵ as $u = u^{(0)} + \epsilon u^{(1)} + O(\epsilon^2)$ yields the perturbation equations:

$$u_t^{(0)} = 0, \quad u_t^{(1)} + u^{(0)} \left(u_x^{(0)}\right)^2 = 0. \tag{4.83}$$

Assuming $U = O(1)$, the boundary conditions are $u^{(0)}(t_0, x) = U(t_0, x),\ u^{(1)}(t_0, x) = 0$. To first order, the perturbation series arising from these is

$$u_1(t, x, t_0) = U - \epsilon(t - t_0) U U_x^2, \tag{4.84}$$

which is clearly singular. The RG equation resulting from applying equation (4.40) is

$$U_{t_0} + \epsilon U U_x^2 = 0, \tag{4.85}$$

but this is just the original DE. Since the perturbation equations are first order the direct hidden scales method will yield an equivalent equation. This shows that the hidden scale symmetry to $O(\epsilon^1)$ is exact, and thus of no help for an approximate solution.

We can instead attempt to solve using another kind of approximate Lie solution symmetry. Extending the manifold to include the perturbation parameter ϵ, and treating it just like an independent variable (figure 6*a*,*b*), permits us to define 'perturbation symmetries', that act directly on ϵ. If such a symmetry can be found, then by constructing the associated finite transformation it is possible to directly convert the unperturbed solution to the general solution to the full differential equation (figure 6*c* shows a geometric analogy).

Exact perturbation symmetries, computed from the DE directly, were first proposed by Kovalev *et al.* [20], and this method was demonstrated to correctly solve various DEs that can also be solved by standard methods. They dubbed them 'renormgroup symmetries' owing to a loose analogy to the CGO RG method. However, as the present paper makes clear, these are distinct from the symmetries that underpin CGO RG, prompting our introduction of the alternative nomenclature 'perturbation symmetries' to avoid potential confusion.

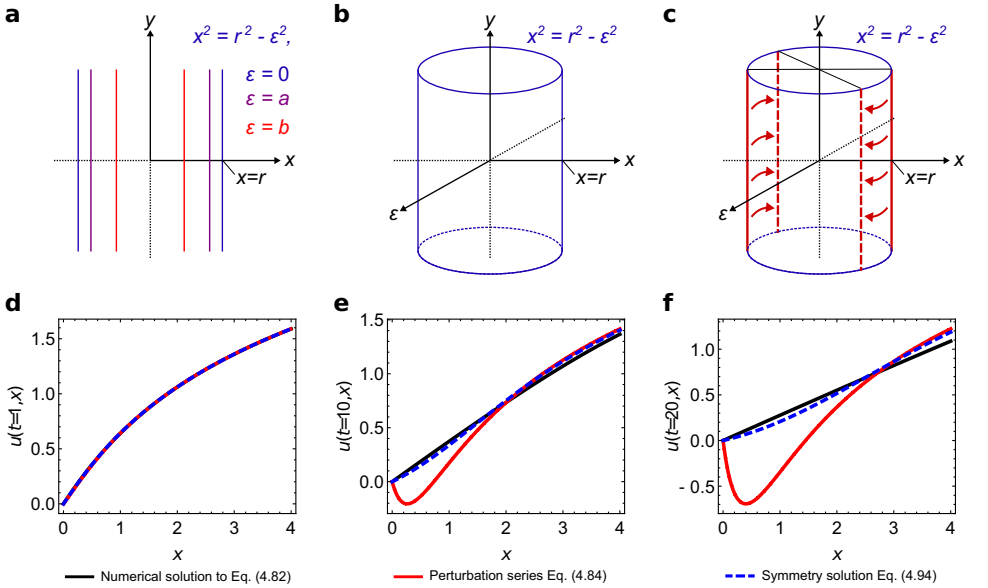

Figure 6. Treating perturbation parameters as variables leads to a richer set of symmetries. (a) Two parallel lines with a perturbation in their distance from the origin have no Lie symmetries. (b) Treating the perturbation parameter as a new variable turns these lines into a cylinder, which has a rotational Lie point symmetry. (c) Any $\epsilon \neq 0$ solution may now be obtained by finite transformation of the $\epsilon = 0$ solution using this symmetry. (d–f) Black: numerical solution of equation (4.82). Red: divergent first-order perturbative solution (equation (4.84)). Blue: first-order approximate manifold generated by perturbation symmetry (equation (4.94)). Solutions evaluated at $t = 1,\ 10$ and 20, respectively.

Approximate perturbation symmetries, calculated laboriously in the traditional way from DEs, were proposed [28] as a perturbation-series-free alternative to CGO RG, although it was not suggested that it could succeed when CGO RG fails. In this article, we have instead taken the opposite approach, that the availability of a perturbation series enables the straightforward computation of these and other kinds of approximate symmetries that would otherwise be extremely laborious or impossible to determine using traditional methods.

One might expect the generator for a zeroth order approximate perturbation symmetry to take the form:

$$X^{(0)} = \sum_{i=1}^{n} \xi_i^{(0)} \frac{\partial}{\partial x_i} + \sum_{j=1}^{m} \eta_j^{(0)} \frac{\partial}{\partial y_j} + \sum_{i=1}^{p} \xi_{c_i}^{(0)} \frac{\partial}{\partial c_i} + \xi_\epsilon^{(0)} \frac{\partial}{\partial \epsilon}, \tag{4.86}$$

where ϵ is the perturbation parameter, and c_i are other constant parameters to which the manifold has been extended. (This approach was taken [28].) However, the derivative with respect to ϵ mixes orders and can be viewed as an $O(\epsilon^{-1})$ operator, inappropriately pulling higher-order terms into the zeroth-order symmetry. The zeroth-order solution to the perturbation problem is the unperturbed solution, and so the zeroth-order symmetries should also be the unperturbed symmetries, which will not be true with the above formulation. Instead, ϵ should be replaced everywhere in the perturbation series with ϵs, where s plays the role of the perturbative switching, running from 0 to 1, and ϵ retains the scale. Seeking approximate perturbation symmetries instead in s then avoids issues of mixing orders. The kth-order term in the generator then takes the form:

$$X^{(k)} = \sum_{i=1}^{n} \xi_i^{(k)} \frac{\partial}{\partial x_i} + \sum_{j=1}^{m} \eta_j^{(k)} \frac{\partial}{\partial y_j} + \sum_{i=1}^{p} \xi_{c_i}^{(k)} \frac{\partial}{\partial c_i} + \xi_s^{(k)} \frac{\partial}{\partial s}. \tag{4.87}$$

Similarly, if c_i are perturbative, they can be replaced with ϵc_i in the DEs, so that c_i are now $O(1)$, and now equation (4.87) no longer mixes orders.

We are now in a position to calculate $O(\epsilon)$ approximate perturbation symmetries for equation (4.82). Since we are not calculating envelope symmetries we no longer need t_0 and can set it to the value for which we know U, say $t_0 = 0$. We first consider ones that act only on x and ϵ. Such symmetries do not act on u directly, so should satisfy the following equation to $O(\epsilon^2)$:

$$(\boldsymbol{X}^{(0)} + \epsilon \boldsymbol{X}^{(1)})(U - \epsilon s t U U_x^2)|_{u=U-\epsilon s t U U_x^2} = 0. \tag{4.88}$$

At zeroth-order this gives $\xi_x^{(0)} = 0$; at first order, we find

$$(\xi_x^{(1)} U_x - \xi_s^{(0)} t U U_x^2)|_{U=u} = 0 \quad \Rightarrow \xi_x^{(1)} = t u U_x \xi_s^{(0)}. \tag{4.89}$$

Thus, the perturbation symmetry is

$$\boldsymbol{X}(x, s) = \xi_s^{(0)} \left(\frac{\partial}{\partial s} + \epsilon t u U_x \frac{\partial}{\partial x} \right). \tag{4.90}$$

Now let $x = H(u)$ be the inverse form of the equation $u = U(x)$. Since s can conveniently be chosen to parameterize it, the corresponding finite transformation is

$$\frac{d\tilde{x}}{ds} = \epsilon t u U_{\tilde{x}} \;\Rightarrow \int_{H(u)}^{x} \frac{d\tilde{x}}{U_{\tilde{x}}} = \epsilon [s]_0^1 t u = \epsilon t u, \tag{4.91}$$

where the limits in the integral follow because when $s = 0$, $u = U(x)$, and therefore $x = H(u)$.

To perform the integral an explicit initial value U is required, whereupon the resultant equation can be solved for u to give a globally valid non-divergent approximate solution. As an example, we consider the initial value $U(x) = \ln(1 + x)$, in which case the perturbation series becomes

$$u = \ln(1 + x) - \epsilon t \frac{\ln(1 + x)}{(1 + x)^2} + O(\epsilon^2), \tag{4.92}$$

and, with $H(u) = e^u - 1$, the integral becomes:

$$\epsilon t u = \left[\frac{1}{2} \tilde{x}^2 + \tilde{x} \right]_{e^u - 1}^{x} = \frac{1}{2} x^2 + x + 1 - e^u - (e^u - 1)^2. \tag{4.93}$$

Some rearrangement gives the approximate symmetry solution as

$$u(t, x) = \frac{1}{2\epsilon t}(x + 1)^2 - \frac{1}{2} W \left[\frac{1}{\epsilon t} e^{(x+1)^2/(\epsilon t)} \right] + O(\epsilon^2), \tag{4.94}$$

where $W[\ldots]$ is the Lambert W-function or the product logarithm. In figure 6*d–f*, we demonstrate that this is indeed a globally valid accurate approximate solution, and also confirm the divergence of the perturbation series.

5. Discussion

The ideas developed in this article raise a variety of further questions, not all of which are directly related to the key theme of the paper, but which are nevertheless interesting. We discuss several of these here and outline potential future research directions to investigate them in more detail.

(a) A potential for unification of approximate methods

Using examples we have demonstrated the basis in approximate Lie symmetries of the method of multiple scales, the Poincare–Lindstedt method, CGO RG and RG/E. All approaches indirectly exploit a class of symmetries that we have coined 'hidden scale symmetries'; all but RG/E involve differing degrees of trial-and-error to do so. We have also shown that these symmetries may

instead be directly identified and integrated to solve singular perturbation problems by using an explicitly Lie theoretic approach.

We have also shown that other kinds of approximate symmetries can be identified and exploited when hidden scale symmetries are not obtainable. We suspect that most singular perturbation methods not examined in this article must also depend in some way on various classes of approximate Lie symmetries. Their explicit reformulation in terms of symmetry transformations may provide technical and conceptual advantages, as we have demonstrated for the methods studied in this article. Moreover, perhaps additional methods might be developed based on exploiting new classes of approximate symmetry not heretofore used. Also, potential links between approximate Lie symmetry and nominally non-perturbative approximate methods such as invariant manifold theory [29] could be investigated in greater depth.

(b) Renormalization group reformulated as approximate Lie symmetry

CGO RG contains coarse-graining/splitting and renormalizing steps because it was developed as an analogy of perturbative RG. Our interpretation for the success of the CGO RG method in solving singular perturbation problems is its identification and exploitation of a class of approximate Lie symmetries of the solution that we have termed 'hidden scale symmetries'. When viewed in light of symmetry transformations the splitting and renormalizing steps are revealed as mostly redundant; their removal simplifies the calculations, particularly when multiple splittings are possible.

Reversing the analogy that was the original inspiration for this technique, this suggests that under certain circumstances, perturbative renormalization group in momentum space may be better understood as an approximate Lie symmetry of the integral studied, hearkening back to the original links between exact renormalization group and traditional Lie theory [6]. In particular, this interpretation can hold only if information is not lost, i.e. the RG transformation is reversible. Therefore, the 'coarse-graining' approach to RG of Kadanoff (and Wilson) does not have a straightforward interpretation in terms of approximate Lie symmetries.

On a related note, we would argue that the equivalence to approximate Lie solution symmetries of the 'envelopes' at the heart of Kunihiro's geometric formulation of RG provides an intuitive interpretation of the latter concept.

(c) Broader applications of our method for calculating symmetries

Our results on singular perturbation theory would not have been possible without developing a new method for calculating approximate Lie symmetries to the solutions of DEs. Any such symmetry that can be calculated via the DE using standard methods can be calculated more easily using our approach (e.g. the perturbation symmetry of the underdamped harmonic oscillator; see the electronic supplementary material, §S6). This may have applications in the field of Lie symmetries extending beyond the present paper.

Symmetries involving the integration constants $\boldsymbol{A}$ can *only* be calculated by our approach. Since $\boldsymbol{A}$ remain unfixed, and change implicitly with the independent variables x, the method can only precisely calculate such symmetries when they act on $\boldsymbol{A}$ and x directly, like hidden scale symmetries do. If the integration constants enter the generator but the symmetry does not act on them directly, additional approximation steps must be taken. For instance, using appropriate trial functions for the integration constants (as was effectively done in equation (4.84)) turns the solution-by-symmetry method into a kind of self-consistent approximate method. Such methods should be the subject of a dedicated future study. Furthermore, our method should in principle find the approximate Lie solution symmetries of other kinds of equations such as algebraic or integral equations; given the great power of these symmetries, we therefore expect that this method may find applications unrelated to DEs in the future.

(d) Advantages and disadvantages of the hidden scale approach and MMS

Both the hidden scale method and CGO RG share the advantage over MMS that scales emerge automatically and need not be guessed. Sometimes, to determine the correct scales using MMS, it is necessary to calculate the perturbation series to inconveniently high order. For instance, in equation (4.70), the fourth-order perturbation series is needed to solve to second order by MMS [9]. On the other hand, sometimes the reverse is true and to get an $O(\varepsilon^n)$ global approximate solution using MMS it is only necessary to compute the perturbation series to $O(\varepsilon^{n-1})$ and then simply to eliminate those components from the *equation* for the $O(\varepsilon^n)$ term that will give rise to divergent components in its solution. With CGO RG and hidden scales, the perturbation series must generally be computed to the same order as that of the desired solution. When the perturbation series is challenging or time-consuming to compute, e.g. for certain partial differential equations, and MMS requires only an $O(\varepsilon^{n-1})$ series, MMS may be the preferred method, despite the need to guess the scales.

PLM has been presented as a more primitive version of MMS, out of which MMS evolved [5]; however, there is a difference: whereas MMS always has a mathematically rigorous basis in hidden scale symmetries, PLM is a viable method only when its implementation serendipitously mirrors that of MMS. So PLM succeeds when it unconsciously exploits hidden scale symmetries, and fails when it attempts to exploit transformations that are not valid symmetries.

Overall, though, we believe the direct hidden scales symmetry method will most often be the best choice. We have demonstrated that it can algorithmically solve problems for which earlier techniques are impractical or require significant guesswork. Our hope is that its greater simplicity, intuitiveness and relative lack of operational ambiguity might encourage more routine attempts to approximately solve differential equations analytically in the future, and as before, continue to complement numerical methods of analysis.

Data accessibility. Supplementary material is available online [30].

Declaration of AI use. We have not used AI-assisted technologies in creating this article.

Authors' contributions. A.J.D.: conceptualization, formal analysis, investigation, methodology, validation, visualization, writing—original draft, writing—review & editing; L.M.: conceptualization, formal analysis, methodology, supervision, writing—original draft, writing—review & editing.

Both authors gave final approval for publication and agreed to be held accountable for the work performed therein.

Conflict of interest declaration. We declare we have no competing interests.

Funding. We acknowledge support from the Lindemann Trust Fellowship, English-Speaking Union (A.J.D.), the MacArthur Foundation (L.M.), the Simons Foundation (L.M.) and the Henri Seydoux Fund (L.M.).

Acknowledgements. We are grateful to Teiji Kunihiro, Nigel Goldenfeld and Julia Rupprecht for providing invaluable feedback on the preprint.

References

1. Olver P. 2000 *Applications of Lie groups to differential equations. Graduate Texts in Mathematics*. New York, NY: Springer.
2. Stephani H. 1990 *Differential equations: their solution using symmetries*. Cambridge, UK: Cambridge University Press.
3. Bender C, Orszag S, Orszag S. 1999 *Advanced mathematical methods for scientists and engineers I: asymptotic methods and perturbation theory*. New York, NY: Springer.
4. He J-H. 1999 Homotopy perturbation technique. *Comput. Methods Appl. Mech. Eng.* **178**, 257–262.
5. Kevorkian J, Cole J. 1996 *Multiple scale and singular perturbation methods*. Applied Mathematical Sciences. New York, NY: Springer.

6. Bogoliubov NN, Shirkov DV. 1959, 1980 *Introduction to the theory of quantized fields*. New York, NY: Interscience–Wiley.
7. Shirkov DV, Kovalev VF. 2001 The Bogoliubov renormalization group and solution symmetry in mathematical physics. *Phy. Rep.* **352**, 219–249. (doi:10.1016/S0370-1573(01)00039-4)
8. Chen LY, Goldenfeld N, Oono Y. 1994 Renormalization group theory for blobal asymptotic analysis. *Phys. Rev. Lett.* **73**, 1311–1315. (doi:10.1103/PhysRevLett.73.1311)
9. Chen LY, Goldenfeld N, Oono Y. 1996 Renormalization group and singular perturbations: multiple scales, boundary layers, and reductive perturbation theory. *Phys. Rev. E* **54**, 376–394. (doi:10.1103/PhysRevE.54.376)
10. Kunihiro T. 1995 A geometrical formulation of the renormalization group method for global analysis. *Progr. Theor. Phys.* **94**, 503–514.
11. Kunihiro T. 1997 The renormalization-group method applied to asymptotic analysis of vector fields. *Prog. Theor. Phys.* **97**, 179–200. (doi:10.1143/PTP.97.179)
12. Lagerstrom PA, Casten R. 1972 Basic concepts underlying singular perturbation techniques. *SIAM Rev.* **14**, 63–120.
13. Hinch EJ. 1991 *Perturbation Methods. Cambridge texts in applied mathematics*. Cambridge, UK: Cambridge University Press.
14. Baikov VA, Gazizov RK, Ibragimov NH. 1988 Approximate symmetries. *Matematicheskii Sbornik* **178**, 435–450.
15. Ibragimov N, Kovalev V. 2009 *Approximate and renormgroup symmetries*. Nonlinear Physical Science. Berlin/Heidelberg, Germany: Springer.
16. Fushchich W, Shtelen W. 1989 On approximate symmetry and approximate solutions of the nonlinear wave equation with a small parameter. *J. Phys. A* **22**, L887.
17. Pakdemirli M, Yürüsoy M, Dolapçı. 2004 Comparison of approximate symmetry methods for differential equations. *Acta Appl. Math.* **80**, 243–271. (doi:10.1023/B:ACAP.0000018792.87732.25)
18. Wiltshire R. 2006 Two approaches to the calculation of approximate symmetry exemplified using a system of advection–diffusion equations. *J. Comput. Appl. Math.* **197**, 287–301. (doi:10.1016/j.cam.2005.11.003)
19. Olver PJ, Rosenau P. 1986 The construction of special solutions to partial differential equations. *Phys. Lett. A* **114**, 107–112. (doi:10.1016/0375-9601(86)90534-7)
20. Kovalev VF, Pustovalov VV, Shirkov DV. 1998 Group analysis and renormgroup symmetries. *J. Math. Phys.* **39**, 1170–1188. (doi:10.1063/1.532374)
21. Michaels TCT, Kusters R, Dear AJ, Storm C, Weaver JC, Mahadevan L. 2019 Geometric localization in supported elastic struts. *Proc. R. Soc. A* **475**, 20190370. (doi:10.1098/rspa.2019.0370)
22. Kunihiro T, Kikuchi Y, Tsumura K. 2022 *Geometrical formulation of renormalization-group method as an asymptotic analysis; with applications to derivation of causal fluid dynamics*. Singapore, Singapore: Springer Singapore. (doi:10.1007/978-981-16-8189-9)
23. Goto Si, Masutomi Y, Nozaki K. 1999 Lie-group approach to perturbative renormalization group method. *Prog. Theor. Phys.* **102**, 471–497. (doi:10.1143/PTP.102.471)
24. Faria LM, Rosales RR. 2017 Equation level matching: an extension of the method of matched asymptotic expansion for problems of wave propagation. *Stud. Appl. Math.* **139**, 265–287. (doi:10.1111/sapm.12183)
25. Veysey J, Goldenfeld N. 2007 Simple viscous flows: from boundary layers to the renormalization group. *Rev. Mod. Phys.* **79**, 883–927. (doi:10.1103/RevModPhys.79.883)
26. Clark WA, Gomes MW, Rodriguez-Gonzalez A, Stein LC, Strogatz SH. 2023 Surprises in a classic boundary-layer problem. *SIAM Review* **65**, 291–315. (doi:10.1137/21M1436087)
27. Roper M, Brenner MP. 2009 A nonperturbative approximation for the moderate Reynolds number Navier–Stokes equations. *Proc. Natl. Acad. Sci. USA* **106**, 2977–2982. (doi:10.1073/pnas.0810578106)
28. Iwasa M, Nozaki K. 2006 A method to construct asymptotic solutions invariant under the renormalization group. *Prog. Theor. Phys.* **116**, 605–613. (doi:10.1143/PTP.116.605)
29. Roberts A. 2020 *Linear algebra for the 21st century*. Oxford, UK: Oxford University Press.
30. Alexander J, Mahadevan L. 2025 Supplementary material from: Approximate Lie symmetries and singular perturbation theory. Figshare. (doi:10.6084/m9.figshare.c.7702285)